ASYMPTOTIC APPROXIMATIONS TO CEV AND SABR MODELS

RICHARD JORDAN* AND CHARLES TIER†

VERSION: 4-8-2010; REVISION: 5-17-2011

Abstract. The problem of pricing, hedging and calibrating equity derivatives in a fast and consistent fashion is considered when the underlying asset does not follow the standard Black- Scholes model but instead the CEV or SABR models. The underlying process in the CEV model has volatility as a deterministic function of the asset price while in the SABR model the volatility as a stochastic function of the asset price. In such situations, trading desks often resort to numerical methods to solve the pricing and hedging problem. This can be problematic for complex models if real-time valuations, hedging and calibration are required. A more efficient and practical alternative is to use a formula even if it is only an approximation. A systematic approach is presented, based on the WKB or ray method, to derive asymptotic approximations yielding simple formulas for the pricing problem. For these models, default may be possible and the original ray approximation is not valid near the default boundary so a modified asymptotic approximation or boundary layer correction is derived. New results are also derived for the standard CEV model and the SABR results. The applicability of the results is illustrated by deriving new analytical approximations for vanilla options based on the CEV and SABR models. The accuracy of the results is demonstrated numerically.

Key words. asymptotic approximations, perturbation methods, deterministic volatility, stochastic volatility, CEV model, SABR model

AMS subject classifications. 34E10, 35C20, 91G80

1. Introduction.

Vanilla exchange-traded and Over-the-Counter (OTC) European options or European futures options are often priced and hedged using the Black-Scholes or Black's model [5, 6], respectively. The derivation of the Black-Scholes or Black's pricing formulas assumes that the asset prices have lognormal distributions and that the volatility is constant, i.e. a pricing formula under Geometric Brownian Motion (GBM). In these models there is a one-to-one relationship between the option prices and the volatility. Thus given option prices across the strikes K and the time to maturity $\tau = T - t$, there is a unique value of the volatility (implied volatility) that yields the prices when used in the pricing formulas. However, this is rarely the case in practice since implied volatilities usually vary with K and τ. In other words, the markets depart from the constant volatility assumption by exhibiting significant downward sloping volatility curves and in some markets the in-the-money (ITM) and out-of-the-money (OTM) options trade at higher implied volatilities than at-the-money (ATM) options. This is referred to as the volatility smile or skew. Typically, although not always, the word skew is reserved for the slope of the volatility/strike function, and smile for its curvature.

To price and hedging, traders and portfolio managers have been trying to address issues such as volatility smiles and skews. One would like to have a consistent estimate of volatility risk, across all the different strikes and maturities for a given option portfolio (e.g. trader's book). The variation of volatility with the strike K essentially means that a different model is being used for each strike. This presents several difficulties when managing large books of options. It is not clear that the delta and vega risks[1] calculated at a given strike are consistent with the same risks across strikes. Also if volatility varies with K, it seems likely that volatility also varies systematically as the asset price changes [17, 18]. Any vega risk arising from

*Quantitative Analytics Group, IntercontinentalExchange Inc., 353 N. Clark Street Suite 3100, Chicago, IL 60654, USA (rjordan@math.uic.edu)

†Department of Applied Mathematics, Illinois Institute of Technology, 10 W. 32nd Street, Chicago, IL 60616, USA (ctier@iit.edu)

[1]For example, the delta and vega of a call price $c = c(F, t)$ are defined as $\partial c/\partial F$ and $\partial c/\partial \sigma$, respectively. They correspond to the sensitivity of the option price to the underlying asset price F and volatility σ.

the systematic change of volatility with the asset price could be hedged more properly (and inexpensively) as delta risk. Finally, it is difficult to know which volatility to use in pricing more exotic options. as observed in [24].

Due to these widely accepted *stylized facts* regarding volatility as described in [10] (e.g. volatility is not constant), the pricing and the robust calibration of a model requires relaxing of the GBM assumption. One approach to account for the skew/smile is to use a single local volatility model that correctly prices options at different strikes without adjustments. Commonly these local volatility models involve a stochastic differential equation (SDE) of the form [17, 18]

$$dF = \sigma(F,t)FdW, \tag{1.1}$$

where $F(t)$ is the forward price of the underlying, $\sigma(F,t)$ is the local volatility that needs to be determined and $W(t)$ is standard Brownian motion. Local volatility models are self-consistent, arbitrage free and can be calibrated to precisely match observed market smiles and skews. They are used in pricing by implementing tree models [18, 16] and are often preferred to the more complicated models for computational reasons. However, there are practical problems with these models.

For example one needs to recover a smooth volatility surface $\sigma(F,t)$ in the model from market prices, i.e. the calibration problem. However, it is not easy to extract a continuous local volatility surface from a few discrete option prices. One remarkable result, due to Dupire [18], is that if call options prices corresponding to all possible strikes and maturities are known in a consistent manner then the local volatility $\sigma(F,t)$ is uniquely determined by the relation

$$\sigma(K,T) = \sqrt{2\left(\frac{\partial c/\partial T}{K^2\partial^2 c/\partial K^2}\right)}. \tag{1.2}$$

Here $c = c(F,t)$ represents the price of a European call at time t with strike K and expiration T. In practice this approach has shortcomings since $\partial c/\partial T$ and $\partial^2 c/\partial K^2$ must be computed using only a finite set of option prices available in the market. Hence interpolation is needed in order to use Dupire's formula and it is by no means obvious how to interpolate the data set in such a way that the radicand remains positive and finite [37]. Further, the result is overly sensitive to the (arbitrary) choice of the interpolation, especially for short maturities ($\tau \ll 1$). This results in poor robustness of the method. Moreover, it has recently been observed [22] that the dynamics of the behavior of smiles and skews predicted by local volatility models is the exact opposite of the behavior observed in the marketplace, i.e. local volatility models predict that the skew moves in the opposite direction to the market level while in reality it moves in the same direction. This leads to extremely poor hedging results and the hedges are often worse than the ones obtained using Black's model. The reason is that these hedges are in fact consistent with the smile moving in the same direction as the market.

Another approach is to specify the form of the local volatility $\sigma(F,t)$. These models fall in the category of level dependent volatility models [1, 2, 12], such as the Constant Elasticity of Variance (CEV) model [12] or power law model [24] in which the volatility is a deterministic function of the underlying asset. Similarly, one can also introduce stochastic volatility [20, 26, 28, 33, 34] such as the Stochastic Alpha Beta Rho (SABR) model [22] or stochastic CEV model. These models can be viewed as extensions of Dupire's local volatility model. They are typically more robust about their set of assumptions, i.e. replacing the assumption of constant volatility with deterministic or stochastic volatility.

The CEV process has the local volatility as a deterministic function of the underlying

asset $\sigma(F,t) = VF^{\beta}$ and is described by the following risk-neutral SDE

$$dF = VF^{\beta+1}dW \tag{1.3}$$

where β is the elasticity of the local volatility and V is the scale parameter. The CEV process was first introduced in [13] for $-1 \leq \beta < 0$ and extended in [19] to the case $\beta > 0$. Note that for $\beta = 0$ we recover the GBM case. It has received attention for several reasons. First, the model is consistent with Black's observation [5] that for $\beta < 0$ the volatility changes are negatively correlated with stock returns often referred to as the *leverage effect*. Empirical evidence supporting the inverse relationship between asset price and volatility is given in [8]. Second, the model is potentially consistent with capturing the observed implied volatility skew within option data for both equity and index options [14]. Third, the model can be calibrated to be consistent with market prices of European options prices using the known analytic option formulas [24, 27, 29]. Thus the CEV process provides an improvement to the traditional GBM model and is a viable model for consistent pricing and risk management of options portfolios.

The SABR model is another interesting alternative model to GBM. It is an extension of the CEV process but with stochastic volatility. It was developed in [22] to capture the dynamics of smile in the interest rate derivatives markets. Here the dynamics of the price of a single underlying $F(t)$ as well as the volatility scale parameter $V(t)$ are stochastic satisfying an SDE of the form

$$\begin{aligned} dF &= VF^{\beta+1}d\widetilde{W}_1 \\ dV &= \nu V dW_2 \end{aligned} \tag{1.4}$$

where $\widetilde{W}_1(t)$ and $W_2(t)$ are correlated Brownian motions with $\mathrm{E}[d\widetilde{W}_1, dW_2] = \rho dt$ and $\rho \in [-1, 1]$. The model is characterized by a local volatility function similar to the one from the CEV, $\sigma(F,t) = VF^{\beta}$, with stochastic scale parameter V, the parameter β restricted to $-1 \leq \beta \leq 1$ [22], ν controls the level of the volatility of the scale parameter, and ρ governs the correlation between the changes in the underlying asset and its scale V. This model reduces to Black's model with $\nu = 0$, $\beta = 0$ and hence $\sigma(F,t) = V$. It also reduces to the CEV model when $\rho = q$ and $\nu = 0$.

A key property of the CEV and SABR models, that is often viewed as either a strength or weakness, is the potential absorption of the processes [13] at the lower boundary $F = 0$ (bankruptcy or default case). Although default case is possible for $\beta < 0$, it has undesirable economic implications, particularly for indices, since *it is inconceivable that there is a significant probability of default for indices*. One can perhaps restrict $\beta \geq -1$ for indices to highlight the very unlikely probability of a highly liquid index to default. Another remedy is to modify the underlying asset process such that default is no longer possible. An example is the CEV by including a minimum asset price level below which the volatility becomes constant [3, 14]. However, for equities, the CEV becomes an attractive model where bankruptcy is more often than not a recurrent event (e.g. financial services or airline industries), although in practice the asset price never reaches zero in case of default but rather a very small value. From a practical point of view we regard the default case as a strength of the models [7, 15, 33]. Also it can play a role in pricing of derivatives. Another possibility is the *shifted* CEV [1] and SABR models with default occurring when the asset price reaches a small positive value instead of zero. This has been shown [30] to overcome some of the above difficulties and provide a practical alternative to the CEV when default is possible.

The popularity of a pricing model is often due to the existence of an exact or approximate pricing formula making it possible to calibrate efficiently and rapidly price and hedge

financial derivatives in a real time environment, e.g. Black's pricing formulas. The more complex the model the harder it is to derive a practical closed form solution that can be easily implemented for pricing and risk management. To implement such models often requires a numerical solution such as lattice methods, numerical integration routines or numerical methods for partial differential equations, e.g. finite difference or element methods. Another robust alternative is a Monte-Carlo simulation for valuation, analysis and risk management. This may be slower to give a price in an intra-day high frequency trading environment for which real time valuation and hedging is required. Therefore without a useful formula, the practical issues of implementation can become problematic for a trader or portfolio manager. The model's lack of practicability hinders its usefulness despite its modeling strengths versus the standard GBM. Analytic formulas would certainly be practical and advisable to look for. Whether they are exact or approximate, they can provide a very fast way to perform real time option hedges obtained by analytically differentiating the pricing formulas. Moreover it makes it possible to calibrate efficiently in a real time environment [44]. The formulas are an improvement over numerical methods such as lattice, numerical integration, PDE or Monte-Carlo methods.

Progress has been made in developing approximate pricing formulas especially with the SABR [22, 23] and CEV model extensions [4, 24]. The SABR model [22], despite its lack of an explicit or *quasi*-closed form solution [23, 25, 32], is popular among practitioners due to the existence of an approximate or asymptotic formula [22, 38] to price European style calls and puts giving good agreement between the theoretical and observed smiles for $\tau \ll 1$. The model allows the market price and the market risks to be obtained immediately using the asymptotic formula. It also provides good and sometimes spectacular fits to the implied volatility curves observed in the marketplace. More importantly, the SABR model captures the correct dynamics of the smile, and thus yields stable hedges. In [23] the authors refine the results from [22] by using a more general asymptotic technique [43] as a method to price derivatives using risk-neutral expectation.

The purpose of this paper is to present a general systematic approach to derive approximate analytic formulas for European type of derivatives based on the CEV and SABR models. In particular, we use the ray method that was developed in the theory of wave propagation [31]. It was applied to general diffusion equations in [9, 41]. The method consists of first constructing an asymptotic solution or ray solution for $\tau \ll 1$ valid away from the boundaries. If necessary a boundary layer solution is constructed in the neighborhood of the boundaries. The ray and boundary layer solutions are then matched to determine any unknown quantities in them. The present method has a number of virtues. First it is general and can be applied to any diffusion equation in any domain. Thus it does not depend upon separability or any other special property of the equation. Second, it provides very useful and accurate quantitative approximations to the probability density function that can be used to price financial derivatives.

The approach taken in this paper differs from that of [4, 22, 23, 24] in several important ways. First we present the ray method as a systematic approach to derive the asymptotic behavior of the density function for $\tau \ll 1$ away from and near the boundaries. Next, we present a general asymptotic method [39] to obtain a uniform approximation to the pricing integral for call and put options and its corresponding deltas. This is illustrated using the CEV and SABR model. Our approximations provide new analytic formulas for pricing European derivative contracts. Finally, by introducing the ray method and the uniform expansion of integrals we present a practical *recipe* of three steps to derive approximate pricing formulas for time to expiration τ small: (1): define an exact risk-neutral expectation integral; (2): derive the asymptotic formula for the probability density function p for small τ; (3): asymptotically

expand the risk-neutral integral with the asymptotic formula for p. The *recipe* provides a practical set of tools needed for pricing and hedging of European contingent claims undertaken with more sophisticated models in a high frequency trading environment.

This paper is organized as follows. In Section 2 we review the CEV process and derive the ray and boundary layer solutions for the risk-neutral density function. We then derive new uniform approximations for the prices of the European call and put options for $\beta \neq 0$. In Section 3 we consider the SABR model and we derive and the ray solution and boundary layer correction for the density function. Again we derive new uniform approximations for the prices of the European call and put options for $\beta \neq 0$. In Section 4 we benchmark the asymptotic formulas from Sections 2 and 3 to standard numerical methods as well to special cases for which an exact solution is known. In addition, a simple calibration is performed using the analytic formulas to illustrate their practicality and speed. Details of the derivations are given in the Appendices and in [29].

2. The CEV Model. We assume that the dynamics of the forward price $F(t)$ are described by the CEV model [13] with the SDE

$$dF = VF^{\beta+1}dW. \tag{2.1}$$

The local volatility is a deterministic function of the underlying asset $\sigma(F,t) = VF^{\beta}$ where $V > 0$ is the deterministic volatility scale parameter and $-\infty < \beta < \infty$ is the elasticity of the local volatility [1, 14]. The risk-neutral density function is defined as $p(\widehat{F}, T, F, t) = \frac{\partial}{\partial \widehat{F}}\Pr\left[F(T) \leq \widehat{F} | F(t) = F\right]$, where $t \in [0,T]$. Here $F = F(t)$ and $\widehat{F} = F(T)$ are the backward and forward variables, respectively. The density function p is needed in our pricing scheme and is a solution of

$$\frac{\partial p}{\partial T} = \frac{1}{2}V^2\frac{\partial^2}{\partial \widehat{F}^2}\left[\widehat{F}^{2\beta+2}p\right], \quad T > t, \qquad \lim_{T\to t} p(\widehat{F}, T, F, t) = \delta(\widehat{F} - F). \tag{2.2}$$

The boundary conditions for (2.2) are not arbitrary since the equation is singular at both $\widehat{F} = 0$ and $\widehat{F} = \infty$ [33, 34]. When $\beta \geq 0$, the boundary at $\widehat{F} = 0$ is a natural boundary while $\widehat{F} = \infty$ is an entrance. When $\beta \leq 0$, $\widehat{F} = \infty$ is a natural boundary. If $-1/2 \leq \beta < 0$, the boundary at $\widehat{F} = 0$ is an exit and the process is absorbed, i.e. default is possible. On the other hand when $\beta < -1/2$, the boundary at $\widehat{F} = 0$ is regular and we impose an absorbing boundary condition. Thus we use the following boundary conditions for (2.2) :

$$\begin{aligned}
&\beta < 0 : p(0,T,F,t) = 0 \quad \text{(absorbing boundary)} \\
&\qquad \lim_{\widehat{F}\to\infty} p(\widehat{F}, T, F, t) = 0 \quad \text{(natural boundary)} \\
&\beta > 0 : p(0,T,F,t) = 0 \quad \text{(natural boundary)} \\
&\qquad \lim_{\widehat{F}\to\infty}\left[\widehat{F}\frac{\partial p}{\partial \widehat{F}}\right] = 0 \quad \text{(entrance boundary)}.
\end{aligned} \tag{2.3}$$

We find the solution of (2.2) for $\beta \neq 0$ with the appropriate boundary conditions in (2.3) to be [1, 33]

$$\begin{aligned}
p(\widehat{F}, T, F, t) = \frac{\widehat{F}^{-2\beta-3/2}F^{1/2}}{V^2|\beta|(T-t)}\exp\left(-\frac{\widehat{F}^{-2\beta} + F^{-2\beta}}{2V^2\beta^2(T-t)}\right) \\
\times I_{1/2|\beta|}\left(\frac{[\widehat{F}F]^{-\beta}}{V^2\beta^2(T-t)}\right)
\end{aligned} \tag{2.4}$$

where $I_\nu(\cdot)$ is the modified Bessel function. If $\beta > 0$, $\widehat{F} = 0$ is a natural boundary and is not accessible and $\widehat{F} = \infty$ is an entrance so that $p(\widehat{F}, T, F, t)$ is a proper density function, i.e.

$$\int_0^\infty p(\widehat{F}, T, F, t) d\widehat{F} = 1. \tag{2.5}$$

It is known that for $\beta > 0$ there is no equivalent martingale measure for F [14, 33]. If $\beta < 0$, $\widehat{F} = 0$ is accessible (exit or regular boundary) and $\widehat{F} = \infty$ is natural so that $p(\widehat{F}, T, F, t)$ does not integrate to one, i.e.

$$\int_0^\infty p(\widehat{F}, T, F, t) d\widehat{F} = 1 - P_0(F, T, t). \tag{2.6}$$

Here $P_0(F, T, t) = \Pr[F(T) = 0 | F(t) = F]$ is the absorption probability at $\widehat{F} = 0$ which we find to be [14, 33]

$$P_0(F, T, t) = \frac{1}{\Gamma[1/(2|\beta|)]} \int_{F^{-2\beta}/2V^2\beta^2(T-t)}^\infty s^{1/(2|\beta|)-1} e^{-s} ds. \tag{2.7}$$

For $\beta < 0$, F is a martingale.

Risk-Neutral Pricing. We assume that the price $u(F, t)$ of a European derivative with payoff function $\Lambda(F)$ is given by

$$u(F, t) = e^{-r(T-t)} \int_0^\infty \Lambda(\widehat{F}) p(\widehat{F}, T, F, t) d\widehat{F}.$$

Here F follows a CEV process so that p is given by (2.4) and r is the constant risk-free interest rate. Unfortunately, computing the integral numerically often proves difficult and/or CPU intensive especially in a trading environment requiring fast computations e.g. algorithmic trading. The next step in our scheme is find an approximation to the density p. We could asymptotically expand (2.4) directly for t near T [30]. Instead we will develop an approximation directly from (2.2) using a perturbation method and then use it in the integral. This approach will be particularly useful when the exact form of p is not available and will motivate our later results on the SABR model. Finally, we obtain our approximation to the price by expanding the above integral asymptotically.

Asymptotic Analysis. We now present our scheme for obtaining approximations to the prices of European derivatives.

We seek an asymptotic solution to the density function p in (2.2) with (2.3) but with $\tau = T - t$ in the form [41, 42]

$$p(F, \widehat{F}, \tau) \sim e^{-\phi^2/4\tau} \sum_{n=0}^\infty Z_n \tau^{n-1/2}, \quad \tau \to 0. \tag{2.8}$$

Here ϕ and Z_n are unknown functions of $\widehat{F}$ and F. The initial condition in (2.2) implies that $\phi = 0$ as $\widehat{F} \to F$. We now substitute (2.8) into (2.2), collect powers of τ to find to leading order

$$\frac{V^2}{2} \widehat{F}^{2\beta+2} \phi_{\widehat{F}}^2 = 1, \quad \phi \to 0 \text{ if } \widehat{F} \to F \tag{2.9}$$

where $\phi_{\widehat{F}}$ denotes partial differentiation with respect to $\widehat{F}$. At the next order we obtain

$$2\widehat{F}^{2\beta+2}\phi_{\widehat{F}}Z_{0,\widehat{F}} + Z_0\left[\widehat{F}^{2\beta+2}\phi_{\widehat{F}\widehat{F}} + 2\left(\widehat{F}^{2\beta+2}\right)_{\widehat{F}}\phi_{\widehat{F}}\right] = 0. \tag{2.10}$$

The solutions of (2.9) and (2.10) are

$$\phi = \frac{\sqrt{2}}{V\beta}\left(F^{-\beta} - \widehat{F}^{-\beta}\right) \text{ and } Z_0 = C\widehat{F}^{-3(\beta+1)/2} \tag{2.11}$$

where C is determined by normalization to be

$$C = \frac{1}{VF^{-(\beta+1)/2}\sqrt{2\pi}}, \qquad \beta \neq 0. \tag{2.12}$$

RESULT 1. *For $\beta \neq 0$ the leading term in the asymptotic solution for p away from the boundaries is given by*

$$p(\widehat{F}, T, F, t) \sim \left(\frac{F}{\widehat{F}^3}\right)^{(\beta+1)/2} \frac{e^{-(F^{-\beta}-\widehat{F}^{-\beta})^2/2V^2\beta^2(T-t)}}{V\sqrt{2\pi(T-t)}}, \quad T-t \to 0. \tag{2.13}$$

To illustrate that the asymptotic solution (2.13) may not satisfy the boundary conditions, which was not taken into account in [25], we set $\beta = -1$ in the exact solution (2.4) to find

$$p = \frac{1}{V\sqrt{2\pi(T-t)}}\left[e^{-\frac{(\widehat{F}-F)^2}{2V^2(T-t)}} - e^{-\frac{(\widehat{F}+F)^2}{2V^2(T-t)}}\right]. \tag{2.14}$$

On the other hand the asymptotic solution in (2.13) for this case is

$$p \sim \frac{e^{-\frac{(\widehat{F}-F)^2}{2V^2(T-t)}}}{V\sqrt{2\pi(T-t)}}, \;\; T-t \to 0. \tag{2.15}$$

Clearly the asymptotic solution does not satisfy the boundary condition in (2.3) for $\beta = -1$, or in fact for other $\beta < 0$, and hence is not complete. The same conclusion applies for the boundary condition in (2.3) for $\beta > 0$. This is characteristic of a *singular perturbation* problem and a boundary layer solution is needed in order to satisfy the boundary conditions.

To construct the boundary layer solution, we introduce the change of variable $\widehat{x} = \widehat{F}^{-2\beta}/[V^2\beta^2]$ into (2.2) leading to

$$\frac{\partial p}{\partial \tau} - \frac{\partial^2}{\partial \widehat{x}^2}\left[2\widehat{x}p\right] + \frac{\partial}{\partial \widehat{x}}\left[\left(2 + \frac{1}{\beta}\right)p\right] = 0 \tag{2.16}$$

where $x = F^{-2\beta}/[V^2\beta^2]$. We first construct a boundary layer solution p_b for $\beta < 0$ near $\widehat{x} = 0$ ($\widehat{F} = 0$) with boundary conditions (2.3) of the form [40]

$$p \sim p_b(x, \widehat{x}, \tau) \equiv \tau^c e^{\phi_0^2/4\tau}\Psi\left(\widehat{\xi}\right), \;\; \widehat{\xi} = \widehat{x}/\tau^2. \tag{2.17}$$

The variable $\widehat{\xi}$ is called the stretched variable and we define $\phi_0 = \phi_{\widehat{x}=0}$ with $\phi = \sqrt{2}(\sqrt{x} - \sqrt{\widehat{x}})$. Substituting (2.17) into (2.16) we find the leading order boundary layer equation to be

$$\left[2\widehat{\xi}\Psi\right]'' - \left(2 + \frac{1}{\beta}\right)\Psi' - \frac{x}{2}\Psi = 0, \;\; \Psi(0) = 0 \tag{2.18}$$

with solution that satisfies the appropriate boundary conditions to be

$$p_b = C_1 \tau^{1/(2\beta)-1} e^{\phi_0^2/4\tau} \widehat{\xi}^{1/(4\beta)} I_{1/(2|\beta|)} \left(\sqrt{x\widehat{\xi}} \right). \tag{2.19}$$

Here C_1 is a constant to be determined by asymptotic matching, i.e. the boundary layer solution must be consistent or match with the asymptotic solution valid away from 0. The matching consists of comparing p_b for $\widehat{\xi} \to \infty$ with (2.13), after the change of variable leading to (2.16), as $\widehat{x} \to 0$ and choosing the unknown constants so that the two expressions agree.

We use the fact that $I_\nu(z) \sim e^z/\sqrt{2\pi z}\,(1+\ldots)$ for $z \gg 1$ which implies that as $\widehat{\xi} \to \infty$ that

$$p_b = C_1 \tau^{1/(2\beta)-1} e^{-x/2\tau} \frac{2^{1/4}}{\sqrt{2\pi}(2x)^{1/4}} \widehat{\xi}^{1/(4\beta)-1/4} e^{(x\widehat{\xi})^{1/2}} (1+\ldots). \tag{2.20}$$

We re-write the boundary layer solution in terms of $\widehat{x}$ so that

$$p_b = C_1 \frac{2^{1/4}}{\sqrt{\pi\tau}(2x)^{1/4}} \widehat{x}^{1/(4\beta)-1/4} e^{-x/2\tau + \sqrt{x\widehat{x}}/\tau} (1+\ldots). \tag{2.21}$$

We then compare it with the leading term (2.13) written in terms of $\widehat{x}$ for $\widehat{x} \ll 1$ which is

$$p \sim \frac{1}{2\sqrt{2\widehat{x}\pi\tau}} \left(\frac{\widehat{x}}{x} \right)^{1/4+1/(4\beta)} e^{-\phi^2/4\tau} \text{ with } \phi = \sqrt{2}\left(\sqrt{x} - \sqrt{\widehat{x}} \right) \sim 2x - 4\sqrt{x\widehat{x}}$$

yielding

$$C_1 = \frac{1}{2x^{1/4\beta}}. \tag{2.22}$$

Since the change of variables leading to (2.16) maps $\widehat{F} = \infty$ into $\widehat{x} = 0$ for $\beta > 0$, the construction of the boundary layer for $\beta > 0$ follows from the analysis for the case $\beta < 0$. We summarize the results for the boundary layer solution using (2.21) and (2.22) in terms of the original variables.

RESULT 2. *For $\beta \neq 0$ the leading term in the boundary layer solution in terms of original variables is given by*

$$\begin{aligned} p_b(\widehat{F}, T, F, t) = \frac{1}{V^2|\beta|(T-t)} \left(\frac{F^{1/2}}{\widehat{F}^{-2\beta+3/2}} \right) e^{-F^{-2\beta}/2\beta^2 V^2 (T-t)} \\ \times I_{1/2|\beta|} \left(\frac{[\widehat{F}F]^{-\beta}}{V^2\beta^2(T-t)} \right), \quad t \to T \end{aligned} \tag{2.23}$$

valid for $\widehat{F} \approx 0$ for $\beta < 0$ and $\widehat{F} \gg 1$ for $\beta > 0$.

The boundary layer solution (2.23) is illustrated in Figure 2.1. The two figures contain the boundary layer solution (2.23) for the density function p, the exact solution (2.4) and the ray solution (2.13), for $\beta = -2$, $V = 0.4$, $T - t = 0.5$ and $\beta = 2$, $V = 0.4$, $T - t = 0.5$. Result 2 provides a more robust approximation than the ray solution near the boundaries by first satisfying the boundary conditions and secondly by being more accurate.

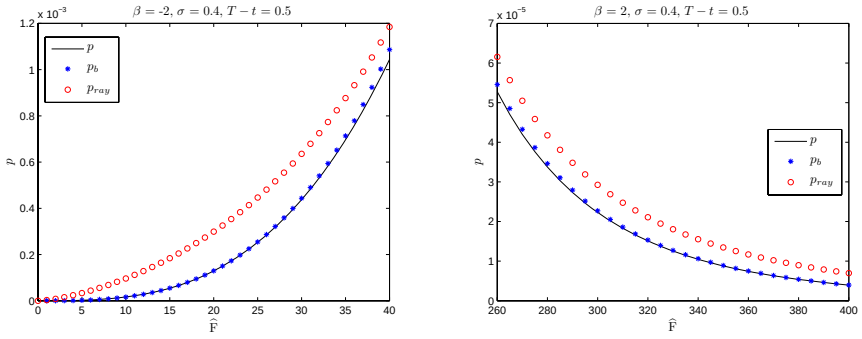

FIG. 2.1. *Illustration of the boundary layer solution (2.23), the exact solution (2.4) and (2.13), for* $\beta = -2$, $V = 0.4$, $T - t = 0.5$ *and* $\beta = 2$, $V = 0.4$, $T - t = 0.5$.

Applications. The integral representation for the price $u(F,t)$ of a European derivative with payoff function $\Lambda(\widehat{F})$ where F follows a CEV process for $\beta > 0$ is given by

$$u(F,t) = e^{-r(T-t)} \int_0^\infty \Lambda(\widehat{F}) p(\widehat{F}, T, F, t) d\widehat{F} \tag{2.24}$$

and for $\beta < 0$ by [33]

$$u(F,t) = e^{-r(T-t)} \int_0^\infty \Lambda(\widehat{F}) p(\widehat{F}, T, F, t) d\widehat{F} + \Lambda(0) P_0(t,F). \tag{2.25}$$

Here p is the density function defined in (2.4) and P_0 is the absorption probability (2.7) at $\widehat{F} = 0$. For a specific payoff function, (2.24) and (2.25) are not straightforward to evaluate and numerical methods are often required. But this does not lead to a simple analytic formula which we would prefer. We obtain a useful approximation to u by replacing p in (2.24) and (2.25) with the approximation (2.13) to obtain

$$u(F,t) \sim e^{-r(T-t)} \int_0^\infty \Lambda(\widehat{F}) \left(\frac{F}{\widehat{F}^3}\right)^{(\beta+1)/2} \frac{e^{-(F^{-\beta}-\widehat{F}^{-\beta})^2/2V^2\beta^2(T-t)}}{V\sqrt{2\pi(T-t)}} d\widehat{F} \tag{2.26}$$

where the absorption probability P_0 is omitted if $\beta < 0$ since it is exponentially small for $T - t \ll 1$ [7].

The approximate price of a European call option $c(F,t)$ for $\beta \neq 0$ is given by (2.26) which becomes

$$c(F,t) \sim e^{-r(T-t)} \int_K^\infty (\widehat{F} - K) \left(\frac{F}{\widehat{F}^3}\right)^{(\beta+1)/2} \frac{e^{-(F^{-\beta}-\widehat{F}^{-\beta})^2/2V^2\beta^2(T-t)}}{V\sqrt{2\pi(T-t)}} d\widehat{F} \tag{2.27}$$

where the payoff function is $\Lambda(F) = \max(F - K, 0)$. We now look at the $\beta < 0$ case and introduce the change of variables $x = (F^{-\beta} - \widehat{F}^{-\beta})/V|\beta|$ in (2.27) to obtain

$$c(F,t) \sim \frac{1}{\sqrt{2\pi(T-t)}} \int_{-\infty}^z f(x) e^{-x^2/2(T-t)} dx, \quad z = \frac{F^{-\beta} - K^{-\beta}}{V|\beta|}. \tag{2.28}$$

Here

$$f(x) = e^{-r(T-t)} \left[\left(F^{-\beta} - xV|\beta|\right)^{-1/\beta} - K \right] F^{(\beta+1)/2} \times \left(F^{-\beta} - xV|\beta|\right)^{(1+1/\beta)/2} \tag{2.29}$$

where $f(0) = e^{-r(T-t)}(F-K)$ and $f(z) = 0$. We now asymptotically expand the integral in (2.28) for $\tau = T-t \ll 1$ using integration by parts to obtain a uniform asymptotic expansion as derived and proven in [39]. We write $f(x) = 1 + [f(x) - 1]$ leading to

$$\begin{aligned} c(z,t) = & \frac{f(0)}{\sqrt{2\pi(T-t)}} \int_{-\infty}^{z} e^{-x^2/2(T-t)} dx \\ & + \sqrt{\frac{T-t}{2\pi}} \left[\frac{f(0) - f(z)}{z} \right] e^{-z^2/2(T-t)} \\ & + \sqrt{\frac{T-t}{2\pi}} \int_{-\infty}^{z} \frac{d}{dx} \left[\frac{f(x) - 1}{x} \right] e^{-x^2/2(T-t)} dx. \end{aligned} \tag{2.30}$$

The leading term in the asymptotic approximation of the call option price for the CEV model for $\beta < 0$ is

$$c(F,t) \sim \frac{f(0)}{\sqrt{2\pi(T-t)}} \int_{-\infty}^{z} e^{-x^2/[2(T-t)]} dx + \sqrt{\frac{T-t}{2\pi}} \left[\frac{f(0) - f(z)}{z} \right] e^{-z^2/2(T-t)}$$

where z and $f(x)$ are defined in (2.28) and (2.29), respectively, leading to

$$\begin{aligned} c(F,t) \sim e^{-r(T-t)} \Bigg\{ & \frac{F-K}{\sqrt{2\pi(T-t)}} \int_{-\infty}^{(F^{-\beta} - K^{-\beta})/V|\beta|} e^{-x^2/2(T-t)} dx + \\ & \frac{(T-t)V|\beta|(F-K)}{F^{-\beta} - K^{-\beta}} \frac{e^{-(F^{-\beta} - K^{-\beta})^2/2(T-t)V^2\beta^2}}{\sqrt{2\pi(T-t)}} \Bigg\}. \end{aligned} \tag{2.31}$$

Performing the same calculations for the put option with $\beta > 0$ leads to the asymptotic pricing formula

$$\begin{aligned} p(F,t) \sim e^{-r(T-t)} \Bigg\{ & \frac{K-F}{\sqrt{2\pi(T-t)}} \left[\int_{-\infty}^{(F^{-\beta} - K^{-\beta})/V|\beta|} e^{-x^2/2(T-t)} dx \right] + \\ & \frac{(T-t)V|\beta|(K-F)}{F^{-\beta} - K^{-\beta}} \frac{e^{-(F^{-\beta} - K^{-\beta})^2/2(T-t)V^2\beta^2}}{\sqrt{2\pi(T-t)}} \Bigg\}. \end{aligned} \tag{2.32}$$

We summarize the asymptotic pricing formulas for the call and put price for $\beta \neq 0$.

RESULT 3. *For $\beta < 0$ and $t \to T$ the asymptotic approximation for the price of a European call option using (2.31) is given by*

$$c(F,t) \sim e^{-r(T-t)} \left\{ (F-K) N(d_{1,cev}) + \left[\frac{F-K}{d_{1,cev}} \right] n(d_{1,cev}) \right\}, \tag{2.33}$$

where

$$d_{1,cev} = \frac{F^{-\beta} - K^{-\beta}}{V|\beta|\sqrt{T-t}} \tag{2.34}$$

and similarly the leading asymptotic approximation for the price of a European put option is given by

$$\begin{aligned} p(F,t) \sim & e^{-r(T-t)} \Bigg\{ (K-F) \left[N(d_{2,cev}) - N(d_{1,cev}) \right] \\ & + (K-F) \left[\frac{n(d_{2,cev})}{d_{2,cev}} - \frac{n(d_{1,cev})}{d_{1,cev}} \right] \Bigg\}. \end{aligned} \tag{2.35}$$

Here

$$d_{2,cev} = \frac{F^{-\beta}}{V|\beta|\sqrt{T-t}}. \tag{2.36}$$

$N(x) = \int_{-\infty}^{x} \frac{e^{-s^2/2}}{\sqrt{2\pi}} ds$ *is the cumulative normal distribution and* $n(x) = \frac{dN(x)}{dx}$ *is the normal density function. The asymptotic approximations for the put and call options for* $\beta > 0$ *and* $t \to T$ *can be obtained in a similar fashion by using (2.32) leading to,*

$$p(F,t) \sim e^{-r(T-t)} \left\{ (K-F)N(d_{1,cev}) + \left[\frac{K-F}{d_{1,cev}} \right] n(d_{1,cev}) \right\}. \tag{2.37}$$

and

$$\begin{aligned} c(F,t) \sim & e^{-r(T-t)} \Bigg\{ (F-K) \left[N(d_{2,cev}) - N(d_{1,cev}) \right] \\ & + (F-K) \left[\frac{n(d_{2,cev})}{d_{2,cev}} - \frac{n(d_{1,cev})}{d_{1,cev}} \right] \Bigg\}. \end{aligned} \tag{2.38}$$

We note that as $d_{2,cev} \to \infty$ or $\beta \to 0$ (2.35) and (2.37) asymptotically satisfy the put-call parity $c(F,t) - p(F,t) \sim (F-K)e^{-r(T-t)}$. Figure 2.2 illustrates the convergence of the put-call parity for $\beta = -2$, $K = 100$, $V = 0.3$, $r = 0.02$ and $T - t = 0.25$. The relative error, defined as the absolute value of the difference between $c(F,t) - p(F,t)$ and $(F-K)e^{-r(T-t)}$ divided by $(F-K)e^{-r(T-t)}$, is less than 0.5%. The asymptotic approximation will become even better for $T - t \ll 1$.

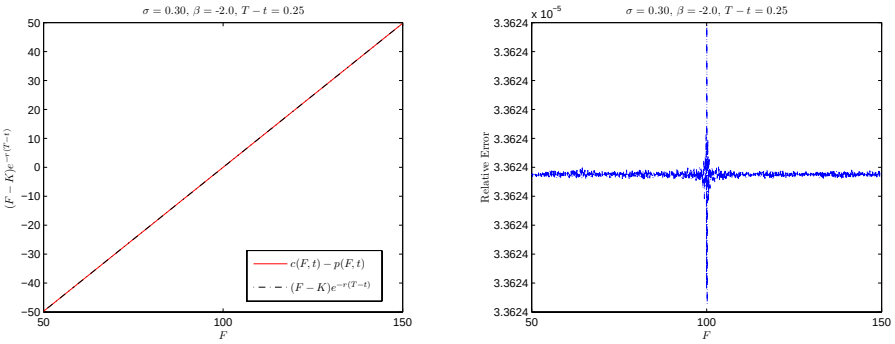

FIG. 2.2. *Illustration of the put-call parity applying equations (2.33) and (2.35) such that* $c(F,t) - p(F,t) \sim (F-K)e^{-r(T-t)}$*, with parameters* $\beta = -2$*,* $K = 100$*,* $V = 0.3$*,* $r = 0.02$ *and* $T - t = 0.25$*.*

We compute the results for the deltas of the call and put prices for $\beta \neq 0$, by differentiating (2.33), (2.35), (2.37) and (2.38), in Result 3. Figure 2.3 illustrates the results for the delta of the call and put price for $\beta < 0$ in equations (2.39) and (2.41). Result 4 below provides the formulas needed to determine the sensitivity of the option price with respect to the underlying asset price F under the CEV model. The combination of Results 3 and 4 provide a basic set of analytic formulas needed to quickly price and hedge option contracts under the CEV model.

RESULT 4. *For* $\beta < 0$ *and* $t \to T$*, the asymptotic approximation for the delta of the price of a European call option using (2.33) is given by*

$$\frac{\partial c}{\partial F}(F,t) \sim e^{-r(T-t)} \left\{ N(d_{1,cev}) + \frac{n(d_{1,cev})}{d_{1,cev}} \right.$$

$$-\frac{(F-K)}{d_{1,cev}^2}\frac{\partial d_{1,cev}}{\partial F}n(d_{1,cev})\Bigg\} \tag{2.39}$$

where

$$\sqrt{T-t}\frac{\partial d_{1,cev}}{\partial F} = \frac{1}{VF}(F^{-\beta}-K^{-\beta}) - \frac{1}{V}F^{-\beta-1} \tag{2.40}$$

and the leading asymptotic approximation for the delta of a European put option using (2.35) is given by

$$\begin{aligned}\frac{\partial p}{\partial F}(F,t) \sim & e^{-r(T-t)}\Bigg\{N(d_{1,cev}) - N(d_{2,cev}) + \frac{n(d_{1,cev})}{d_{1,cev}} \\ & -\frac{n(d_{2,cev})}{d_{2,cev}} + \frac{(K-F)}{d_{1,cev}^2}\frac{\partial d_{1,cev}}{\partial F}n(d_{1,cev})\Bigg\}.\end{aligned} \tag{2.41}$$

The asymptotic approximations for the delta of the put and call options for $\beta > 0$ and $t \to T$ can be obtained in a similar fashion by using (2.37) leading to,

$$\begin{aligned}\frac{\partial p}{\partial F}(F,t) \sim & \; e^{-r(T-t)}\Bigg\{-N(d_{1,cev}) + \frac{n(d_{1,cev})}{d_{1,cev}} \\ & -\frac{(K-F)}{d_{1,cev}^2}\frac{\partial d_{1,cev}}{\partial F}n(d_{1,cev})\Bigg\}\end{aligned} \tag{2.42}$$

and, using (2.38),

$$\begin{aligned}\frac{\partial c}{\partial F}(F,t) \sim & e^{-r(T-t)}\Bigg\{-N(d_{1,cev}) + N(d_{2,cev}) - \frac{n(d_{1,cev})}{d_{1,cev}} \\ & +\frac{n(d_{2,cev})}{d_{2,cev}} - \frac{(F-K)}{d_{1,cev}^2}\frac{\partial d_{1,cev}}{\partial F}n(d_{1,cev})\Bigg\}.\end{aligned} \tag{2.43}$$

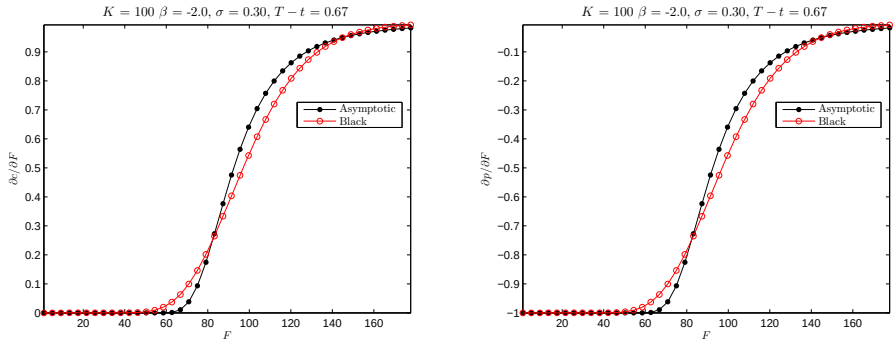

FIG. 2.3. *Illustration of the delta for the call and put price applying equations (2.39) and (2.41) with parameters $\beta = -2$, $K = 100$, $V = 0.3$, $r = 0.0$ and $T - t = 3/4$ versus the delta under Black's model.*

3. SABR Model. We now consider the stochastic CEV or SABR model [22, 25] in which the forward price of the asset $F = F(t)$ as well as the volatility scale parameter $V = V(t)$ are stochastic and follow (1.4) or equivalently

$$\begin{aligned} dF &= \sqrt{1-\rho^2} V F^{\beta+1} dW_1 + \rho V F^{\beta+1} dW_2 \\ dV &= \nu V dW_2 \end{aligned} \tag{3.1}$$

where $\widetilde{W_1}(t) = \sqrt{1-\rho^2} W_1(t) + \rho W_2(t)$ and $W_1(t)$ and $W_2(t)$ are uncorrelated standard Brownian motions. The local volatility function is $\sigma(F,t) = VF^\beta$ where β is not restricted to $-1 \le \beta \le 1$ as in [22]. The parameter ν controls the level of the volatility of the scale parameter V and ρ governs the correlation between the changes in the underlying asset and V. We now use our three step pricing scheme, as applied to the CEV model above. We first concentrate on the density function

$$p = p(\widehat{F}, \widehat{V}, T, F, V, t) = \frac{\partial}{\partial \widehat{F}} \text{Pr}[F(T) \le \widehat{F}, V(T) \le \widehat{V} | F(t) = F, V(t) = V]$$

where F, V, t are the backward variables and $\widehat{F} = F(T)$,$\widehat{V} = V(T)$,T are the forward variables, that satisfies the following forward equation

$$\frac{\partial p}{\partial T} = \frac{1}{2}\widehat{V}^2 \frac{\partial^2}{\partial \widehat{F}^2}\left[\widehat{F}^{2\beta+2} p\right] + \frac{1}{2}\nu^2 \frac{\partial^2}{\partial \widehat{V}^2}\left[\widehat{V}^2 p\right] + \rho\nu \frac{\partial^2}{\partial \widehat{F} \partial \widehat{V}}\left[\widehat{V}^2 \widehat{F}^{\beta+1} p\right], \tag{3.2}$$

with $\widehat{F},\ \widehat{V} > 0$ and initial condition

$$\lim_{T-t \to 0} p(\widehat{F}, \widehat{V}, T, F, V, t) = \delta(\widehat{F} - F)\delta(\widehat{V} - V). \tag{3.3}$$

Again, the boundary conditions for (3.2) may not be arbitrary since the equation is singular at both $\widehat{F} = 0,\ \infty$ and $\widehat{V} = 0,\ \infty$. We believe, based on the CEV model in (2.2), that $\widehat{F} = 0$ is absorbing and $\widehat{F} = \infty$ is natural if $\beta < 0$, while $\widehat{F} = 0$ is natural and $\widehat{F} = \infty$ is an entrance if $\beta > 0$. Also $\widehat{V} = 0$, $\widehat{V} = \infty$ are natural for all β. Thus we use the following boundary conditions for (3.2) with (3.3) :

$$\begin{aligned} \beta < 0 :\ & p(0, \widehat{V}, T, F, V, t) = 0 \ \text{(absorbing)}, \ \lim_{\widehat{F} \to \infty} p(\widehat{F}, \widehat{V}, T, F, V, t) = 0 \quad \text{(natural)} \\ & p = 0 \quad \text{(natural)}, \quad \widehat{V} = 0,\ \infty \quad \text{(natural)} \\ \beta > 0 :\ & p(0, \widehat{V}, T, F, V, t) = 0 \ \text{(natural)}, \ \lim_{\widehat{F} \to \infty} \left[\widehat{F} \frac{\partial p}{\partial \widehat{F}}\right] = 0 \quad \text{(entrance)} \\ & p = 0 \quad \text{(natural)}, \quad \widehat{V} = 0,\ \infty \quad \text{(natural)}. \end{aligned} \tag{3.4}$$

For $\beta = 0$ all the boundaries are natural.

We now present some special cases of the SABR model for which exact solutions are available.

McKean Problem. McKean [35] considered the problem of diffusion on the Poincaré plane (surface of negative curvature) which is a special case of the SABR model (3.2) with $\rho = 0$, $\beta = -1$ but in the right-half plane, i.e the domain of $\widehat{F}$ is extended to be $-\infty < \widehat{F} < \infty$. If we define $y = F\ \widehat{y} = \widehat{F}$, $x = V/\nu$, $\widehat{x} = \widehat{V}/\nu$, $\tau = \nu^2(T-t)/2$ in (3.2) then the McKean density function, $p_{mk} = p_{mk}(\widehat{x}, \widehat{y}, x, y, \tau)$ satisfies the problem in [35]

$$\frac{\partial p_{mk}}{\partial \tau} = \frac{\partial^2}{\partial \widehat{y}^2}\left[\widehat{x}^2 p_{mk}\right] + \frac{\partial^2}{\partial \widehat{x}^2}\left[\widehat{x}^2 p_{mk}\right], \quad \lim_{\tau \to 0} p_{mk} = \delta(\widehat{x} - x)\delta(\widehat{y} - y). \tag{3.5}$$

McKean constructed the solution to (3.5) in the right half plane $\widehat{x} > 0$ and $-\infty < \widehat{y} < \infty$ with the boundary condition

$$p_{mk} = 0 \quad \text{on all boundaries}, \tag{3.6}$$

as

$$p_{mk} = \frac{e^{-\tau/4}\sqrt{2}}{(4\pi\tau)^{3/2}\widehat{x}^2} \int_{\phi}^{\infty} \frac{ze^{-z^2/4\tau}}{\sqrt{\cosh(z) - \cosh(\phi)}} dz, \tag{3.7}$$

where

$$\phi = \cosh^{-1}\left(1 + \frac{(x-\widehat{x})^2 + (y-\widehat{y})^2}{2\widehat{x}x}\right).$$

The function ϕ represents the geodesic distance from $(\widehat{x}, \widehat{y})$ to (x, y) on the Poincaré plane. However, the density function p_{mk} in (3.7) is not a solution of the SABR problem (3.2)-(3.4), written in terms of $x, \widehat{x}$, $y, \widehat{y}$ and τ with $\rho = 0$, $\beta = -1$, since it is not on the proper domain and does not satisfy the boundary condition for the SABR density $p = 0$ if $\widehat{y} = 0$ ($\widehat{F} = \infty$). However, as noted in [23] one can construct $p = p(\widehat{x}, \widehat{y}, x, y, \tau)$ using p_{mk} with the proper boundary condition by means of the method of images

$$p = p_{mk}(\widehat{x}, \widehat{y}, x, y, \tau) - p_{mk}(\widehat{x}, \widehat{y}, x, -y, \tau). \tag{3.8}$$

Correlated McKean Problem. Another special case related to the McKean problem is the SABR model with $\beta = -1$ and $\rho \neq 0$. Introducing the same change of variables to obtain (3.5), (3.2) becomes

$$\begin{aligned} \frac{\partial p_{cmk}}{\partial \tau} &= \frac{\partial^2}{\partial \widehat{y}^2}\left[\widehat{x}^2 p_{cmk}\right] + \frac{\partial^2}{\partial \widehat{x}^2}\left[\widehat{x}^2 p_{cmk}\right] + 2\rho \frac{\partial^2}{\partial \widehat{x}\partial \widehat{y}}\left[\widehat{x}^2 p_{cmk}\right], \\ \lim_{\tau \to 0} p_{cmk} &= \delta(\widehat{y} - y)\delta(\widehat{x} - x) \end{aligned} \tag{3.9}$$

where $x, \widehat{x}$, $y, \widehat{y}$ and τ are defined above. The density function p_{cmk} in the right half plane satisfying the boundary conditions (3.6) was given in [23] as

$$p_{cmk} = \frac{e^{-\tau/4}\sqrt{2}}{(4\pi\tau)^{3/2}\widehat{x}^2\sqrt{1-\rho^2}} \int_{\phi}^{\infty} \frac{ze^{-z^2/4\tau}}{\sqrt{\cosh(z) - \cosh(\phi)}} dz, \tag{3.10}$$

with

$$\phi = \cosh^{-1}\left(1 + \frac{(x-\widehat{x})^2 + 2\rho(x-\widehat{x})(y-\widehat{y}) + (y-\widehat{y})^2}{2(1-\rho^2)\widehat{x}x}\right).$$

Similarly, we construct the SABR density function p by the method of images in (3.8) after restricting the domain to the first quadrant and then using the boundary condition at $\widehat{y} = 0$. We now summarize the results for the special SABR cases for which an exact integral solution is known. These special cases will be used to illustrate the accuracy of our asymptotic solutions.

RESULT 5. *The solution to the SABR model (3.2) with $\beta = -1$ and all ρ using (3.10) and the method of images in (3.8), is*

$$\begin{aligned} p = \frac{e^{-\nu^2(T-t)/8}}{2[\pi(T-t)]^{3/2}\nu^2\widehat{V}^2\sqrt{1-\rho^2}} \Bigg\{ &\int_{\phi}^{\infty} \frac{ze^{-z^2/2\nu^2(T-t)}}{\sqrt{\cosh(z) - \cosh(\phi)}} dz - \\ &\int_{\phi_i}^{\infty} \frac{ze^{-z^2/2\nu^2(T-t)}}{\sqrt{\cosh(z) - \cosh(\phi_i)}} dz \Bigg\}, \end{aligned} \tag{3.11}$$

with

$$\begin{aligned}\phi &= \cosh^{-1}\left(1+\frac{(V-\widehat{V})^2-2\rho V\nu(V-\widehat{V})(F-\widehat{F})+\nu^2(F-\widehat{F})^2}{2(1-\rho^2)\widehat{V}V}\right),\\ \phi_i &= \cosh^{-1}\left(1+\frac{(V-\widehat{V})^2-2\rho V\nu(V-\widehat{V})(F+\widehat{F})+\nu^2(F+\widehat{F})^2}{2(1-\rho^2)\widehat{V}V}\right).\end{aligned} \tag{3.12}$$

Here ϕ and ϕ_i represent geodesic distances between $(\widehat{x},\widehat{y})$ and (x,y) in the Poincaré plane.

The absorbing boundary condition for the SABR model in (3.4) is related to the one in the CEV model for $\beta<0$ in (2.6). Therefore, having an absorbing boundary condition results in the total mass of the density function being less than one

$$\int_0^\infty\int_0^\infty p(\widehat{F},\widehat{V},T,F,V,t)d\widehat{V}d\widehat{F}<1, \qquad \beta<0.$$

Similar to the CEV process in that we must define the absorption probability at $\widehat{F}=0$, $P_0(F,T,V,t)=\mathrm{Pr}[F(T)=0|F(t)=F]$.

Despite the existence of an exact solution for the density function for these special cases, the integral in (3.11) must still be evaluated numerically to price derivatives. The value of European options based on the SABR model in Result 5 requires integration of the payoff function times the density function (3.11). A different view that reduces the number of integrations in the pricing integral is to use the marginal density $p^F=\displaystyle\int_0^\infty p\,d\widehat{V}$.

Finally, we observe that the SABR solution in (3.11) with $\beta=-1$, $\rho=0$ and $\nu\to 0$ can be simplified to the special case of the Bachelier model. Integrating (3.11) over $\widehat{V}$, to derive the marginal distribution $p^F=p^F(\widehat{F},T,F,t)$, and taking the limit $\nu\to 0$, leads to

$$p^F=\frac{1}{V\sqrt{2\pi(T-t)}}e^{-(\widehat{F}-F)^2/2V^2(T-t)}. \tag{3.13}$$

Risk-Neutral Pricing. We illustrate the pricing of European style derivatives by considering the price $u(F,t)$ with payoff function $\Lambda(F)$ for $\beta>0$ given by

$$u(F,t)=e^{-r(T-t)}\int_0^\infty\int_0^\infty \Lambda(\widehat{F})p\,d\widehat{V}d\widehat{F}=e^{-r(T-t)}\int_0^\infty \Lambda(\widehat{F})p^F\,d\widehat{F} \tag{3.14}$$

and for $\beta<0$ by

$$u(F,t)=e^{-r(T-t)}\int_0^\infty \Lambda(\widehat{F})p^F\,d\widehat{F}+\Lambda(0)P_0(t,F) \tag{3.15}$$

where p^F is the marginal density function and P_0 is the absorption probability at $\widehat{F}=0$. The formulas in (3.14) and (3.15) are an exact integral representation for a variety of European style derivatives such as the call option if $\Lambda(F)=\max(F-K,0)$. For a specific payoff function (3.14) and (3.15) may be difficult to evaluate and numerical methods are often required. But this does not lead to a simple analytic formula which we would prefer. As in Section 2 we develop analytic approximations directly from (3.2) with (3.3) and boundary conditions in (3.4). The results are derived using the same systematic approach but now no exact solution is available for p.

Asymptotic Analysis. For the uncorrelated SABR model with $\rho = 0$, $\beta \neq 0$, and the correlated SABR model with $\rho \neq 0$, $\beta \neq 0$, the exact solution for the density function p in (3.2) is not known so we will construct approximations. Following our approach for the CEV model, we seek an asymptotic solution of (3.2) for small $\tau = T - t$. The form of a ray solution [41, 42] is

$$p \sim p_{ray} \equiv e^{-\phi^2/2\nu^2\tau} \sum_{n=0}^{\infty} Z_n \tau^{n-1}, \qquad \tau \ll 1 \tag{3.16}$$

where ϕ and Z_n are to be determined. The initial condition in (3.3) implies that the leading term in the series is τ^{-1} and $\phi = 0$, $Z_0 = 1$ as $\widehat{F} \to F$ and $\widehat{V} \to V$. We now substitute (3.16) into (3.2), collect powers of τ and equate the coefficients of each power of τ to zero. After introducing

$$\widehat{x} = \frac{\widehat{V}}{\nu}, \quad \text{and} \quad \widehat{y} = \frac{F^{-\beta}}{\beta} \tag{3.17}$$

we obtain the following eikonal equation at $\mathcal{O}(\tau^{-3})$

$$\widehat{x}^2 \left[\phi_{\widehat{y}}^2 + \phi_{\widehat{x}}^2 - 2\rho \phi_{\widehat{x}} \phi_{\widehat{y}} \right] = 1. \tag{3.18}$$

From the coefficients of τ^{-2} together with (3.18), we obtain the transport equation

$$\begin{aligned} & 2\widehat{x} \left[\phi_{\widehat{y}} Z_{0,\widehat{y}} + \phi_{\widehat{x}} Z_{0,\widehat{x}} - \rho \phi_{\widehat{x}} Z_{0,\widehat{y}} - \phi_{\widehat{y}} Z_{0,\widehat{x}} \right] \\ & + Z_0 \left[\widehat{x}^2 \left(\phi_{\widehat{yy}} + \phi_{\widehat{xx}} - \rho \phi_{\widehat{xy}} - \rho \phi_{\widehat{yx}} \right) \right. \\ & \left. - \frac{\widehat{x}^2 (\beta+1)}{\widehat{y}\beta} \phi_{\widehat{y}} - \frac{2\widehat{x}^2 (\beta+1)}{\widehat{y}\beta} \left(\phi_{\widehat{y}} - \rho \phi_{\widehat{x}} \right) + 4\widehat{x} \left(\phi_{\widehat{x}} - \rho \phi_{\widehat{y}} \right) - \frac{1}{\phi} \right] = 0. \end{aligned} \tag{3.19}$$

We solve (3.18) and (3.19) by the method of characteristics, as sketched in Appendix A, leading to the earlier result

$$\phi = \cosh^{-1} \left(1 + \frac{(x - \widehat{x})^2 + 2\rho(x - \widehat{x})(y - \widehat{y}) + (y - \widehat{y})^2}{2(1 - \rho^2)\widehat{x}x} \right). \tag{3.20}$$

Given the solution to the eikonal equation, we now solve for the transport equation (3.19) which can be written as a first order differential equation, along a ray or characteristic, as

$$\begin{aligned} & \frac{dZ_0}{d\phi} + Z_0 \left[\frac{1}{2} \widehat{x}^2 \left(\phi_{\widehat{yy}} + \phi_{\widehat{xx}} - \rho \phi_{\widehat{xy}} - \rho \phi_{\widehat{yx}} \right) \right. \\ & \left. - \frac{\widehat{x}^2 (\beta+1)}{2\widehat{y}\beta} \phi_{\widehat{y}} - \frac{\widehat{x}^2 (\beta+1)}{\widehat{y}\beta} \left(\phi_{\widehat{y}} - \rho \phi_{\widehat{x}} \right) + 2\widehat{x} \left(\phi_{\widehat{x}} - \rho \phi_{\widehat{y}} \right) - \frac{1}{2\phi} \right] = 0. \end{aligned}$$

The steps for finding Z_0 are sketched in Appendix B. The ray solution, after a tedious calculation in Appendix B, can be expressed as

$$\begin{aligned} p_{ray} = & -\frac{e^{-\phi^2/2\nu^2\tau}}{2\pi\tau\widehat{x}^2\nu^2\sqrt{1-\rho^2}} \sqrt{\frac{\phi}{\sinh(\phi)}} \left(\frac{\widehat{y}}{y} \right)^{(\beta+1)/(2\beta)} \\ & \times \exp\left[-\frac{\rho(\beta+1)}{2\beta} \int_0^{\phi} H(z) dz \right], \end{aligned} \tag{3.21}$$

where ϕ is defined in (3.20) and

$$H(z) \equiv \frac{\widehat{x}^2(z)\phi_{\widehat{x}}(z)}{\widehat{y}(z)}. \tag{3.22}$$

The negative sign in the ray solution in (3.21) arises from the change of variable $\widehat{y} = \widehat{F}^{-\beta}/\beta$ leading to $d\widehat{y} = -\widehat{F}^{-\beta-1}d\widehat{F}$. In addition, the solution to the integral $\int_0^\phi H(z)dz$ is sketched in Appendix C. We now summarize the results.

RESULT 6. *The leading term ray solution, for $t \to T$, of the SABR model in its original variables, based on (3.21) with (C.3), (C.6) and (C.7), is given by*

$$\begin{aligned} p_{ray}(\widehat{F},\widehat{V},T,F,V,t) = {} & \frac{e^{-\phi^2/2\nu^2(T-t)}}{2\pi\nu(T-t)\widehat{V}^2\widehat{F}^{\beta+1}\sqrt{1-\rho^2}}\sqrt{\frac{\phi}{\sinh(\phi)}}\left(\frac{\widehat{F}}{F}\right)^{-(\beta+1)/2} \\ & \times \exp\left[-\frac{\rho(\beta+1)}{2\beta}\Phi(\widehat{F},\widehat{V})\right], \end{aligned} \tag{3.23}$$

where

$$\begin{aligned} \phi = \cosh^{-1}\Bigg(1 & \\ & + \frac{\beta^2(V-\widehat{V})^2 + 2\rho\nu\beta(V-\widehat{V})(F^{-\beta}-\widehat{F}^{-\beta}) + \nu^2(F^{-\beta}-\widehat{F}^{-\beta})^2}{2\beta^2(1-\rho^2)\widehat{V}V}\Bigg), \end{aligned} \tag{3.24}$$

$$\Phi(\widehat{F},\widehat{V}) = \frac{2}{\sqrt{1-\rho^2}}\left\{\tan^{-1}\left(e^{\Upsilon}\right) - \tan^{-1}\left(e^{-\phi+\Upsilon}\right)\right\} + \frac{2}{\sqrt{\Omega^2(1-\rho^2)-1}} \tag{3.25}$$

$$\begin{aligned} & \times \left\{\tan^{-1}\left(\frac{\left(\Omega\sqrt{1-\rho^2}+\rho\right)\tanh(\Upsilon/2) - \sqrt{1-\rho^2}}{\sqrt{\Omega^2(1-\rho^2)-1}}\right)\right. \\ & \left. - \tan^{-1}\left(\frac{\left(\Omega\sqrt{1-\rho^2}+\rho\right)\tanh([-\phi+\Upsilon]/2) - \sqrt{1-\rho^2}}{\sqrt{\Omega^2(1-\rho^2)-1}}\right)\right\} \end{aligned} \tag{3.26}$$

and

$$\begin{aligned} \Omega = \frac{1}{\sinh(\phi)}\Bigg\{ & \frac{F^{-\beta}}{\beta}\left[\frac{\rho}{\nu}(V-\widehat{V}) + \frac{1}{\beta}(F^{-\beta}-\widehat{F}^{-\beta})\right] - \frac{\widehat{V}\rho}{\nu\beta}(F^{-\beta}-\widehat{F}^{-\beta}) \\ & - \left[\frac{\beta^2(V^2-\widehat{V}^2) - \nu^2(F^{-\beta}-\widehat{F}^{-\beta})^2}{2\beta^2\nu^2}\right]\Bigg\}, \end{aligned} \tag{3.27}$$

$$\begin{aligned} \Upsilon = \sinh^{-1}\Bigg(\frac{1}{\sqrt{1-\rho^2}} & \\ \times \left[\frac{\beta^2(V^2-\widehat{V}^2) - \nu^2(F^{-\beta}-\widehat{F}^{-\beta})^2 - 2\beta\nu\rho(F^{-\beta}-\widehat{F}^{-\beta}+\beta\rho)(V-\widehat{V})}{2\beta V[\beta\rho(V-\widehat{V}) + \nu(F^{-\beta}-\widehat{F}^{-\beta})]}\right]\Bigg). \end{aligned} \tag{3.28}$$

We will now compare our result with the asymptotic approximation of the exact solution to the McKean problem (3.10) away from the boundary. We follow [23] and use a change of variables of the form $w = [z^2 - \phi^2]/[2\nu^2(T-t)]$ in (3.10) and expand the integrand in powers of $(T-t)$. Integrating over w leads to $p_{ray,cmk}$, the leading term ray solution of the correlated McKean density function

$$p_{ray,cmk}(\widehat{F},\widehat{V},T,F,V,t) = \frac{e^{-\phi_{cmk}^2/2\nu^2(T-t)}}{2\pi\nu(T-t)\widehat{V}^2\sqrt{1-\rho^2}}\sqrt{\frac{\phi_{cmk}}{\sinh(\phi_{cmk})}}$$

with $\phi_{cmk} = \phi|_{\beta=-1}$ defined in (3.24). Equation (3.29) corresponds to the ray solution (3.23) by setting $\beta = -1$.

We note that the underlying asset in the SABR model follows a CEV type process where the scale parameter V is stochastic and correlated with the asset price F. The scale parameter goes from being deterministic in the CEV process to stochastic in the SABR model. In addition V is correlated with F with correlation ρ. From a modeling point of view the leverage effect relates the negative correlation between the changes of the asset price to its volatility. As noted in [38] the leverage effect is related to the steepening effect of the implied volatility curve capture by the parameters $\beta < 0$ and/or $\rho < 0$, so β and ρ play against each other. The market practice is to fix either of the two parameters and optimize on the other. The variable V operates as the scale parameter of the local volatility, $\sigma(F,t) = VF^\beta$, for $\beta \neq 0$. Thus for $\rho = 0$ the change in the volatility scale parameter is uncorrelated to the change in the underlying asset, however the local volatility $\sigma(F,t) = VF^\beta$ is not uncorrelated with the underlying asset. Given that the forward price is governed by the CEV process, the leverage effect can still be captured by β for $T - t \ll 1$.

In order to show qualitatively that the correlation between V and F for $T - t \ll 1$ does not necessarily enhance the modeling of the leverage effect, we perform Monte Carlo (MC) experiment for the following cases: (1) $\rho = 0.0$, $\beta = -2$, (2) $\rho = -0.9$, $\beta = -2$, with $T - t = 1/12$. The first step of the MC experiment consists of simulating 10,000 correlated and uncorrelated outcomes for F and V drawn from (3.1) with (1) $\rho = 0.0$ and (2) $\rho = -0.9$, respectively. The first two plots in Figure 3.1 illustrate the first step of the MC simulation for both cases assuming $\beta = -2$ and $\nu = 0.2$. The next step consist of mapping the simulated outcomes of F against $\sigma = VF^\beta$. This is illustrated in the last two plots in Figure 3.1 (two right hand plots) for which the simulation in the 3rd and 4th plot provide a correlation estimate of approximately -0.90 and -0.98 between F and V, respectively. It clearly shows that the addition of the correlation $\rho = -0.9$ between V and F increases the leverage effect which can also be achieved by making the β more negative, for $T - t \ll 1$. We will focus our attention on the uncorrelated SABR model, i.e. the case $\rho = 0$, in what follows. For the remaining of the paper we do not set $\beta = -1/2$ and optimize ρ, but rather set $\rho = 0$, optimize β and relax the condition $-1 < \beta < 1$ for $T - t \ll 1$.

For completeness we also note that the asymptotic solution may not satisfy the boundary conditions, which was not taken into account in [22, 23, 25]. If we set $\beta = -1$ in the leading term ray solution (3.23) we find

$$p_{ray} = \frac{e^{-\phi^2/2\nu^2(T-t)}}{2\pi\nu(T-t)\widehat{V}^2\sqrt{1-\rho^2}}\sqrt{\frac{\phi}{\sinh(\phi)}}. \tag{3.29}$$

Taking the limit as $\widehat{F} \to 0$ yields

$$p_{ray} = \frac{e^{-{\phi_0}^2/2\nu^2(T-t)}}{2\pi\nu(T-t)\widehat{V}^2\sqrt{1-\rho^2}}\sqrt{\frac{\phi_0}{\sinh(\phi_0)}}, \qquad \phi_0 = \phi|_{\widehat{F}=0}.$$

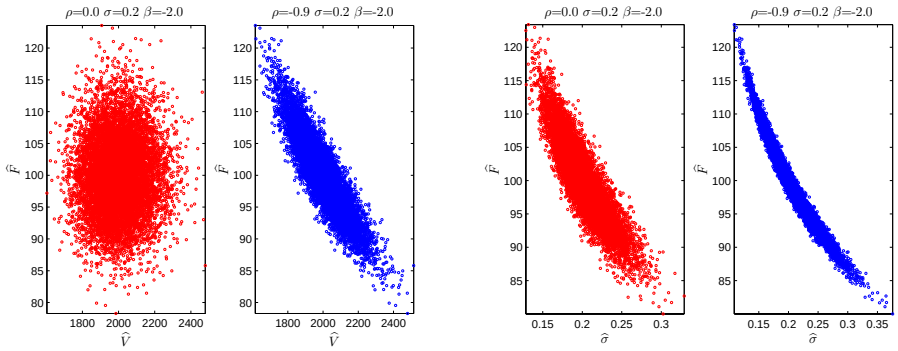

FIG. 3.1. *Monte Carlo experiment for the SABR Model. Simulation of outcomes for $\widehat{F}$ and $\widehat{V}$ (two left hand side plots) and corresponding outcomes of $\widehat{V} = \widehat{V}F^{\beta}$ (two right hand side plots) for $\rho = 0$ and $\rho = -0.9$ assuming $\beta = -2$, $F = 100$, $\nu = 0.2$ and $V = 0.2$.*

Clearly the asymptotic solution does not satisfy the boundary condition in (3.4) for $\beta = -1$, or in fact for other $\beta < 0$. Similarly, for $\beta > 0$ the boundary condition in (3.4) is not satisfied for $\widehat{F} = \infty$.

To construct the boundary layer solution for the SABR model for the case $\beta < 0$ and $\rho = 0$ we introduce

$$\tau = T - t, \qquad \widehat{y} = \frac{\widehat{F}^{-2\beta}}{\beta^2} \tag{3.30}$$

into (3.2) then the density $p = p(\widehat{y}, \widehat{V}, y, V, \tau)$ satisfies

$$\frac{\partial p}{\partial \tau} - \frac{\partial^2}{\partial \widehat{y}^2}\left[2\widehat{V}^2\widehat{y}p\right] + \frac{\partial}{\partial \widehat{y}}\left[\left(2 + \frac{1}{\beta}\right)\widehat{V}^2 p\right] - \frac{\partial^2}{\partial \widehat{V}^2}\left[\frac{\nu^2\widehat{V}^2}{2}p\right] = 0. \tag{3.31}$$

The ray solution now becomes

$$p_{ray} = \frac{e^{-\phi^2/2\nu^2\tau}}{4\pi\tau\nu\widehat{V}^2\sqrt{\widehat{y}}}\sqrt{\frac{\phi}{\sinh(\phi)}}\left(\frac{\widehat{y}}{y}\right)^{(\beta+1)/(4\beta)}. \tag{3.32}$$

We introduce the stretched variable $\widehat{\xi} = \widehat{y}/\tau^2$ into (3.31) leading to

$$\frac{\partial p}{\partial \tau} - \frac{\partial^2}{\partial \widehat{\xi}^2}\left[2\widehat{V}^2\frac{\widehat{\xi}}{\tau^2}p\right] + \frac{\partial}{\partial \widehat{y}}\left[\left(2 + \frac{1}{\beta}\right)\frac{\widehat{V}^2}{\tau^2}p\right] - \frac{\partial^2}{\partial \widehat{V}^2}\left[\frac{\nu^2\widehat{V}^2}{2}p\right] = 0, \tag{3.33}$$

along with the boundary condition (3.4) at $\widehat{\xi} = 0$ and a matching condition described in Appendix D. We assume a boundary layer solution of the form

$$p \sim p_b \equiv \tau^c e^{-\theta(\widehat{V})/\tau}\Psi(\widehat{\xi}) \tag{3.34}$$

where θ is a function of $\widehat{V}$ and Ψ is a function $\widehat{\xi}$. Substituting (3.34) into (3.31) we find the leading order boundary layer equation is

$$\left[\widehat{\xi}\Psi\right]_{\widehat{\xi}\widehat{\xi}} - \left\{\left[\left(1 + \frac{1}{2\beta}\right)\right]\Psi\right\}_{\widehat{\xi}} + \left[\frac{\nu^2\theta_{\widehat{V}}^2}{4} - \frac{\theta}{2\widehat{V}^2}\right]\Psi = 0, \quad \beta < 0,\ \rho = 0, \tag{3.35}$$

with the condition $\Psi(0) = 0$. The solution to (3.35), sketched in Appendix D, leads to the boundary layer solution

$$p_b = \frac{e^{-\phi_0^2/2\nu^2\tau}}{2\sqrt{2\pi}\tau^{3/2}\widehat{V}^2\nu\sqrt{V\widehat{V}}}\left(\frac{\phi_0}{\sinh(\phi_0)}\right)\left(\frac{\widehat{y}}{y}\right)^{1/4\beta} \times I_{1/2|\beta|}\left(\frac{1}{\tau V\widehat{V}}\left(\frac{\phi_0}{\sinh(\phi_0)}\right)\sqrt{y\widehat{y}}\right). \tag{3.36}$$

We now summarize the results for the boundary layer solution term in the original variables using (3.36). In the transformed problem for $\beta > 0$ $\widehat{F} = \infty$ maps into $\widehat{y} = 0$ and the construction of the boundary layer for $\beta > 0$ follows from the analysis for the case $\beta < 0$.

RESULT 7. *The boundary layer solution for the uncorrelated SABR model with $\rho = 0$ and $\beta \neq 0$ in terms the original variables is*

$$p \sim p_b = \frac{\widehat{F}^{-2\beta-1}e^{-\phi_0^2/[2\nu^2(T-t)]}}{|\beta|\nu\sqrt{2\pi}(T-t)^{3/2}\widehat{V}^2\sqrt{V\widehat{V}}}\left(\frac{\widehat{F}}{F}\right)^{-1/2}\left(\frac{\phi_0}{\sinh(\phi_0)}\right) \times I_{1/(2|\beta|)}\left(\frac{(F\widehat{F})^{-\beta}}{(T-t)\beta^2 V\widehat{V}}\left(\frac{\phi_0}{\sinh(\phi_0)}\right)\right) \tag{3.37}$$

where

$$\phi_0 = \cosh^{-1}\left(1 + \frac{(V-\widehat{V})^2 + \nu^2 F^{-2\beta}/\beta^2}{2V\widehat{V}}\right)$$

for $\widehat{F} \approx 0$ for $\beta < 0$ and $\widehat{F} \gg 1$ for $\beta > 0$ under the case $T - t \to 0$.

We demonstrate the accuracy of the boundary layer solution near $\widehat{F} = 0$, for $\beta = -1$. Using the identity $I_{1/2}(z) = \sinh(z)\sqrt{2/\pi z}$, we find

$$p_b = \frac{e^{-\phi_0^2/[2\nu^2(T-t)]}}{\pi\nu(T-t)\widehat{V}^2}\sqrt{\frac{\phi_0}{\sinh(\phi_0)}}\sinh\left(\frac{(F\widehat{F})}{(T-t)V\widehat{V}}\left(\frac{\phi_0}{\sinh(\phi_0)}\right)\right) \tag{3.38}$$

where

$$\phi_0 = \cosh^{-1}\left(1 + \frac{(V-\widehat{V})^2 + \nu^2 F^2}{2V\widehat{V}}\right)$$

for $\widehat{F} \to 0$ and $T - t \to 0$. Figure 3.2 compares a slice of the bivariate density in (3.29) near the boundary $\widehat{F} = 0$, the boundary layer approximation in (3.38) and the numerical approximation to the exact integral solution for $\beta = -1$ in (3.7) in the original variables. The integral was computed numerically with MATLAB© using the recursive adaptive Simpson quadrature. The relative error uses the numerical approximation as the exact result. It is important to note that the boundary layer solution will become even better for $T - t \ll 1$. The figure also illustrates the smooth transition between the boundary layer solution and the ray solution.

Recall that the pricing formulas in (3.14) or (3.15) are expressed in terms of the marginal distribution $p^F = p^F(\widehat{F}, T, F, t)$. We now derive an asymptotic formula for the marginal density function using

$$\begin{aligned} p^F(\widehat{F}, T, F, t) &= \int_0^\infty p(\widehat{F}, \widehat{V}, T, F, V, t)d\widehat{V}, \\ &\sim \int_0^\infty p_{ray}(\widehat{F}, \widehat{V}, T, F, V, t)d\widehat{V}. \end{aligned}$$

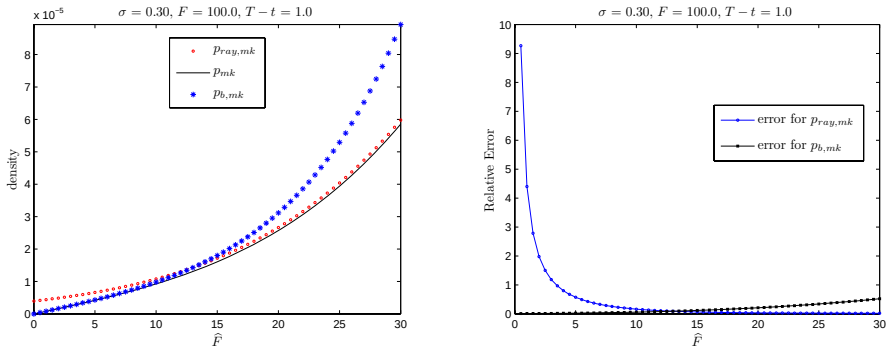

FIG. 3.2. *Comparison between the boundary layer solution in (3.38), the ray solution in (3.23) and the numerical approximation of the exact solution for* $\beta = -1$ *in (3.8) with* $\sigma(F,t) = 0.30$ *with* $F = 100$ *and* $T - t = 1.0$.

where $p_{ray} = p_{ray}(\widehat{F}, \widehat{V}, T, F, V, t)$ is the leading term in the ray solution (3.23) with $\rho = 0$ which is

$$p_{ray} = \frac{1}{2\pi\nu(T-t)\widehat{V}^2\widehat{F}^{\beta+1}}\sqrt{\frac{\phi}{\sinh(\phi)}}\left(\frac{\widehat{F}}{F}\right)^{-(\beta+1)/2} e^{-\phi^2/2\nu^2(T-t)}. \tag{3.39}$$

The derivation of the asymptotic marginal density function is sketched in Appendix E and is given by

$$\begin{aligned} p^F \sim & \frac{1}{\sqrt{2\pi(T-t)}\widehat{V}_{\max}\widehat{F}^{\beta+1}}\sqrt{\frac{V}{\widehat{V}_{\max}}} \\ & \times\left(\frac{\widehat{F}}{F}\right)^{-(\beta+1)/2} e^{-\phi_{\max}^2/2\nu^2(T-t)}, \qquad T-t\to 0 \end{aligned} \tag{3.40}$$

where

$$\widehat{V}_{\max} = \sqrt{V^2 + \frac{\nu^2}{\beta^2}(F^{-\beta} - \widehat{F}^{-\beta})^2}, \quad \phi_{\max} = \cosh^{-1}\left(\frac{\widehat{V}_{\max}}{V}\right).$$

The asymptotic approximation (3.40) of the marginal distribution function is illustrated in Figure 3.3 with different values for β. We now summarize the results for the asymptotic approximation to the marginal density function p^F when $\beta \neq 0$ and $\rho = 0$.

RESULT 8. *The asymptotic behavior of the marginal distribution for the SABR model with* $\rho = 0$ *and* $\beta \neq 0$ *is*

$$\begin{aligned} p^F \sim p^F_{ray} = & \frac{1}{\sqrt{2\pi(T-t)}\widehat{V}_{\max}\widehat{F}^{\beta+1}}\sqrt{\frac{V}{\widehat{V}_{\max}}} \\ & \left(\frac{\widehat{F}}{F}\right)^{-(\beta+1)/2} e^{-\phi_{\max}^2/2\nu^2(T-t)}, \qquad T-t\to 0, \end{aligned} \tag{3.41}$$

where

$$\widehat{V}_{\max} = \sqrt{V^2 + \frac{\nu^2}{\beta^2}(F^{-\beta} - \widehat{F}^{-\beta})^2}, \quad \phi_{\max} = \cosh^{-1}\left(\frac{\widehat{V}_{\max}}{V}\right).$$

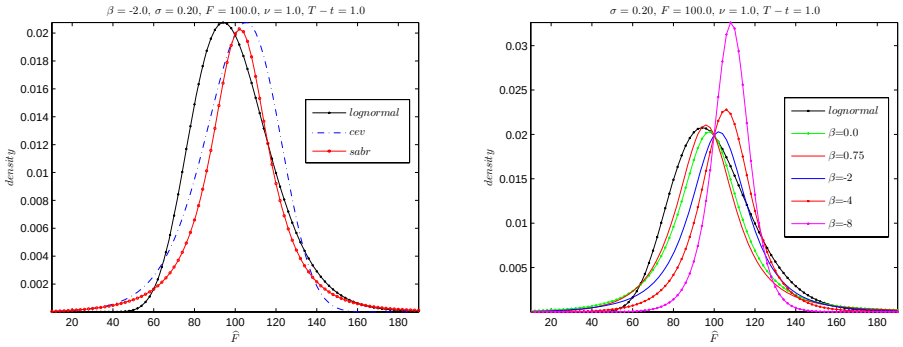

FIG. 3.3. *The left plot illustrates the comparison between (3.40) with* $\beta = -2$, $\sigma(F,t) = 0.2$ *and* $\nu = 1.0$ *and the following two limits: 1)* $\nu = 0$ *(CEV model) and 2)* $\nu = 0$, $\beta = 0$ *(Black's model). The right plot illustrates the asymptotic behavior of* $p^F \sim p^F_{ray}$ *in (3.40) for different values of* β, *for* $\nu = 1.0$, $F = 100$, $T - t = 1.0$ *and* $\sigma(F,t) = 0.2$ *in addition to lognormal case.*

For the special case with $\beta = -1$ we find that

$$p^F_{ray} = \frac{1}{\sqrt{2\pi(T-t)}\widehat{V}_{\max}}\sqrt{\frac{V}{\widehat{V}_{\max}}}e^{-\phi^2_{\max}/2\nu^2(T-t)}, \qquad T - t \to 0,$$

with $\widehat{V}_{\max} = \sqrt{V^2 + \nu^2(F-\widehat{F})^2}$. Computing the marginal density for this special case in the limit $\nu \to 0$ agrees with the marginal density given in (3.13).

Applications. We now derive approximate pricing formulas for European call and put option prices. The integral representation for the price of a European derivative with payoff $\Lambda(\widehat{F})$ is given in (3.14) or (3.15) as

$$u(F,t) = e^{-r(T-t)}\int_0^\infty \Lambda(\widehat{F})p^F d\widehat{F}.$$

Here we omitted the small default probability P_0. We replace p^F by its asymptotic approximation p^F_{ray} to obtain

$$u(F,t) \sim e^{-r(T-t)}\int_0^\infty \Lambda(\widehat{F})p^F_{ray}d\widehat{F}, \quad T - t \ll 1.$$

The prices of European call and put, $c(F,t)$ and $p(F,t)$ are then given by the asymptotic pricing formulas,

$$\begin{aligned} c(F,t) &\sim e^{-r(T-t)}\int_0^\infty \max(\widehat{F}-K,0)p^F_{ray}d\widehat{F} \\ p(F,t) &\sim e^{-r(T-t)}\int_0^\infty \max(K-\widehat{F},0)p^F_{ray}d\widehat{F}. \end{aligned} \tag{3.42}$$

Using the asymptotic marginal density function (3.41) in (3.42), we find the price of the call option to be

$$c(F,t) \sim e^{-r(T-t)}\int_K^\infty (\widehat{F}-K)\frac{1}{\sqrt{2\pi(T-t)}\widehat{V}_{\max}\widehat{F}^{\beta+1}}\sqrt{\frac{V}{\widehat{V}_{\max}}} \left(\frac{\widehat{F}}{F}\right)^{-(\beta+1)/2} e^{-\phi^2_{\max}/2\nu^2(T-t)}d\widehat{F}.$$

We now repeat the analysis in Section 2 to obtain an asymptotic expansion of the integral for $T-t \ll 1$. We let $\widehat{y} = \widehat{F}^{-\beta}/\beta$ to obtain

$$c(y,t) \sim e^{-r(T-t)} \int_{-\infty}^{K^{-\beta}/\beta} ((\widehat{y}\beta)^{-1/\beta} - K) \frac{1}{\sqrt{2\pi(T-t)}\widehat{V}_{\max}} \sqrt{\frac{V}{\widehat{V}_{\max}}} \left(\frac{\widehat{y}}{y}\right)^{(\beta+1)/2\beta} e^{-\phi_{\max}^2/2\nu^2(T-t)} d\widehat{y}$$

with $\widehat{y} = \widehat{F}^{-\beta}/\beta$, $y = F^{-\beta}/\beta$, $\widehat{V}_{\max} = \sqrt{V^2 + \nu^2(y-\widehat{y})^2}$ and $\phi_{\max} = \cosh^{-1}\left(\widehat{V}_{\max}/V\right)$. $\phi_{max} \in [1, \infty)$. $\phi_{\max}$ can be rewritten as

$$\phi_{\max} = \cosh^{-1}\left(\sqrt{1 + \frac{\nu^2}{V^2}(y-\widehat{y})^2}\right) = \ln\left(\frac{\widehat{V}_{\max}}{V} + \frac{\nu}{V}(y-\widehat{y})\right).$$

Now we define $z = \phi_{\max}/\nu$ to get $\widehat{V}_{\max} = V\cosh(\nu z)$, $\widehat{y} = y - \frac{V}{\nu}\sinh(\nu z)$ and

$$d\widehat{y} = -\frac{\widehat{V}_{\max}\sqrt{\widehat{V}_{\max}^2 - V^2}}{\nu(y-\widehat{y})}dz = -\frac{V\cosh(\nu z)\sqrt{\cosh^2(\nu z) - 1}}{\sinh(\nu z)}dz = -V\cosh(\nu z)dz$$

leading to the formula

$$c(z,t) \sim e^{-r(T-t)} \int_{-\infty}^{z} \left(\left(\beta\left[y + \frac{V}{\nu}\sinh(\nu\chi)\right]\right)^{-1/\beta} - K\right) \times \frac{1}{\sqrt{\cosh(\nu\chi)}}\left(1 + \frac{V\sinh(\nu\chi)}{\nu y}\right)^{(\beta+1)/2\beta} \frac{e^{-\chi^2/2(T-t)}}{\sqrt{2\pi(T-t)}}d\chi$$

where

$$z = -\cosh^{-1}(\sqrt{1 + \nu^2/V^2(y - K^{-\beta}/\beta)^2})/\nu. \tag{3.43}$$

The above integral is in the same form as (2.28)

$$c(z,t) \sim \frac{1}{\sqrt{2\pi(T-t)}} \int_{-\infty}^{z} f(x) e^{-x^2/2(T-t)} dx$$

but with

$$f(\chi) = e^{-r(T-t)} \left(\left(\beta\left[y + \frac{V}{\nu}\sinh(\nu\chi)\right]\right)^{-1/\beta} - K\right) \times \frac{1}{\sqrt{\cosh(\nu\chi)}}\left(1 + \frac{V\sinh(\nu\chi)}{\nu y}\right)^{(\beta+1)/2\beta}, \tag{3.44}$$

where $f(0) = e^{-r(T-t)}\left((\beta y)^{-1/\beta} - K\right)$ and $f(z) = 0$. As in Section 2, We use integration by parts with $f(x) = 1 + [f(x) - 1]$ to obtain a uniform asymptotic expansion, derived and proven in [39], as

$$c(z,t) = \frac{f(0)}{\sqrt{2\pi(T-t)}} \int_{-\infty}^{z} e^{-x^2/[2(T-t)]} dx$$

$$+\sqrt{\frac{T-t}{2\pi}}\left[\frac{f(0)-f(z)}{z}\right]e^{-z^2/[2(T-t)]} \tag{3.45}$$
$$+\sqrt{\frac{T-t}{2\pi}}\int_{-\infty}^{z}\frac{d}{dx}\left[\frac{f(x)-1}{x}\right]e^{-x^2/[2(T-t)]}dx.$$

Retaining only the leading term we find an asymptotic formula for the call option price with $\beta < 0$ to be

$$c(z,t) \sim \frac{f(0)}{\sqrt{2\pi(T-t)}}\int_{-\infty}^{z} e^{-x^2/[2(T-t)]}dx$$
$$+\sqrt{\frac{T-t}{2\pi}}\left[\frac{f(0)-f(z)}{z}\right]e^{-z^2/[2(T-t)]}.$$

Here z and $f(z)$ are defined in (3.43) and (3.44), respectively. In terms of the original variables, we find the formula to be

$$c(F,t) \sim e^{-r(T-t)}\left\{\frac{(F-K)}{\sqrt{2\pi(T-t)}}\int_{-\infty}^{z} e^{-x^2/[2(T-t)]}dx\right. \tag{3.46}$$
$$\left.-\left[\frac{(T-t)(F-K)}{z}\right]\frac{e^{-z^2/[2(T-t)]}}{\sqrt{2\pi(T-t)}}\right\}.$$

Repeating the same calculations for the put option with $\beta > 0$ leads to the asymptotic pricing formula

$$p(F,t) \sim e^{-r(T-t)}\left\{\frac{(K-F)}{\sqrt{2\pi(T-t)}}\int_{-\infty}^{-z} e^{-x^2/[2(T-t)]}dx\right. \tag{3.47}$$
$$\left.+\left[\frac{(T-t)(K-F)}{z}\right]\frac{e^{-z^2/[2(T-t)]}}{\sqrt{2\pi(T-t)}}\right\}.$$

The asymptotic formulas for c with $\beta > 0$ and p with $\beta < 0$ are found in a similar fashion. We summarize the asymptotic pricing formulas for the call and put price for $\beta \neq 0$ by using (3.45), (3.46) and (3.47).

RESULT 9. *For $\beta < 0$ and $t \to T$, the leading term asymptotic formulas for the prices of European call and put options using (3.46) are given by*

$$c(F,t) \sim e^{-r(T-t)}\left\{(F-K)N(d_{1,sabr}) + \left[\frac{F-K}{d_{1,sabr}}\right]n(d_{1,sabr})\right\} \tag{3.48}$$

where

$$d_{1,sabr} = \frac{\mathrm{sgn}(\beta)}{\nu\sqrt{T-t}}\ln\left(\sqrt{1+\frac{\nu^2}{V^2\beta^2}(F^{-\beta}-K^{-\beta})^2} + \frac{\nu}{V\beta}(F^{-\beta}-K^{-\beta})\right), \tag{3.49}$$

and

$$p(F,t) \sim e^{-r(T-t)}\left\{(K-F)\left[N(d_{2,sabr}) - N(d_{1,sabr})\right]\right. \tag{3.50}$$
$$\left.+(K-F)\left[\frac{n(d_{2,sabr})}{d_{2,sabr}} - \frac{n(d_{1,sabr})}{d_{1,sabr}}\right]\right\}$$

where

$$d_{2,sabr} = \frac{\text{sgn}(\beta)}{\nu\sqrt{T-t}} \ln\left(\sqrt{1+\frac{\nu^2 F^{-2\beta}}{V^2\beta^2}} + \frac{\nu}{V\beta}F^{-\beta}\right).$$

Here $N(x) = \int_{-\infty}^{x} \frac{e^{-s^2/2}}{\sqrt{2\pi}} ds$ *is the cumulative normal distribution and* $n(x) = \frac{dN(x)}{dx}$ *is normal density functions.*

The asymptotic approximations for the put and call options for $\beta > 0$ *and* $t \to T$ *can be obtained in a similar manner leading to*

$$p(F,t) \sim e^{-r(T-t)}\left\{(K-F)N(d_{1,sabr}) + \left[\frac{K-F}{d_{1,sabr}}\right] n(d_{1,sabr})\right\}, \tag{3.51}$$

and, using (3.45),

$$\begin{aligned} c(F,t) \sim e^{-r(T-t)}\Bigg\{&(F-K)\left[N(d_{2,sabr}) - N(d_{1,sabr})\right] + \\ &\left[\frac{F-K}{d_{2,sabr}}\right] n(d_{2,sabr}) - \left[\frac{F-K}{d_{1,sabr}}\right] n(d_{1,sabr})\Bigg\}, \end{aligned} \tag{3.52}$$

where $\text{sgn}(\beta)$ *represents the sign of* β*, i.e. plus or minus sign.*

We note that as $d_{2,sabr} \to \infty$ or $\beta \to 0$ (3.48) and (3.50) asymptotically satisfy the put-call parity $c(F,t) - p(F,t) = (F-K)e^{-r(T-t)}$. Also (3.48), (3.50), (3.51) and (3.52) in Result 9 have the same explicit form as the formulas (2.33), (2.35), (2.37) and (2.38) in Result 3 for the CEV process. The difference between the SABR and CEV equations arise from the form of the variables $d_{1,sabr}$, $d_{2,sabr}$ and $d_{1,cev}$, $d_{2,cev}$. Taking the limit of $d_{1,sabr}$ in (3.49) for $\nu \to 0$ leads to $d_{1,cev}$ in (2.34) as follows

$$\begin{aligned} \lim_{\nu\to 0} \frac{\text{sgn}(\beta)}{\nu\sqrt{T-t}} \ln\left(\sqrt{1+\frac{\nu^2}{V^2\beta^2}(F^{-\beta}-K^{-\beta})^2} + \frac{\nu}{V\beta}(F^{-\beta}-K^{-\beta})\right) = \\ \text{sgn}(\beta)\frac{F^{-\beta}-K^{-\beta}}{V\beta\sqrt{T-t}}. \end{aligned} \tag{3.53}$$

Here $\text{sgn}(\beta)\beta = |\beta|$ so that (3.53) is equal to (2.34). In addition, for $\beta = -1$, i.e. the Bachelier model, we recover the exact solution by substituting β with negative one in (3.53) for (3.48).

In Result 10 below, we find formulas for the deltas of the call and put prices for $\beta \neq 0$ by differentiating (3.48), (3.50), (3.51) and (3.52). Figure 3.4 illustrates the results for the deltas of the call and put price for $\beta < 0$ in equations (3.54) and (3.56). The combination of Results 9 and 10 provide a basic set of analytical formulas needed to quickly price and hedge option contracts in a stochastic volatility framework for $T - t \ll 1$.

RESULT 10. *For* $\beta < 0$ *and* $t \to T$*, the asymptotic approximation for the delta of the price of a European call option using (3.48) is given by*

$$\begin{aligned} \frac{\partial c}{\partial F}(F,t) \sim e^{-r(T-t)}\Bigg\{&N(d_{1,sabr}) + \frac{n(d_{1,sabr})}{d_{1,sabr}} \\ &-\frac{(F-K)}{d_{1,sabr}^2}\frac{\partial d_{1,sabr}}{\partial F} n(d_{1,sabr})\Bigg\} \end{aligned} \tag{3.54}$$

where

$$\frac{\partial d_{1,sabr}}{\partial F} = \left[\frac{\nu^2(F^{-\beta}-K^{-\beta})^2 - \nu^2 F^{-\beta}(F^{-\beta}-K^{-\beta})}{V^2\beta F\sqrt{1+\nu^2(F^{-\beta}-K^{-\beta})^2/V^2\beta^2}}\right.$$
$$\left. + \frac{\nu}{VF}(F^{-\beta}-K^{-\beta}) - \frac{\nu}{V}F^{-\beta-1}\right] \tag{3.55}$$
$$\Bigg/ \operatorname{sgn}(\beta)\nu\sqrt{T-t}\left[\sqrt{1+\frac{\nu^2}{V^2\beta^2}(F^{-\beta}-K^{-\beta})^2} + \frac{\nu}{V\beta}(F^{-\beta}-K^{-\beta})\right]$$

and the leading asymptotic approximation for the delta of a European put option using (3.50) is given by

$$\frac{\partial p}{\partial F}(F,t) \sim e^{-r(T-t)}\Bigg\{N(d_{1,sabr}) - N(d_{2,sabr})$$
$$+\frac{n(d_{1,sabr})}{d_{1,sabr}} - \frac{n(d_{2,sabr})}{d_{2,sabr}} + \frac{(K-F)}{d_{1,sabr}^2}\frac{\partial d_{1,sabr}}{\partial F}n(d_{1,sabr})\Bigg\}. \tag{3.56}$$

The asymptotic approximations for the delta of the put and call options for $\beta > 0$ and $t \to T$ can be obtained in a similar fashion by using (3.51) leading to,

$$\frac{\partial p}{\partial F}(F,t) \sim e^{-r(T-t)}\left\{-N(d_{1,sabr}) + \frac{n(d_{1,sabr})}{d_{1,sabr}}\right.$$
$$\left. - \frac{(K-F)}{d_{1,sabr}^2}\frac{\partial d_{1,sabr}}{\partial F}n(d_{1,sabr})\right\} \tag{3.57}$$

and, using (3.52),

$$\frac{\partial c}{\partial F}(F,t) \sim e^{-r(T-t)}\Bigg\{ - N(d_{1,sabr}) + N(d_{2,sabr})$$
$$-\frac{n(d_{1,sabr})}{d_{1,sabr}} + \frac{n(d_{2,sabr})}{d_{2,sabr}} + \frac{(F-K)}{d_{1,sabr}^2}\frac{\partial d_{1,sabr}}{\partial F}n(d_{1,sabr})\Bigg\}. \tag{3.58}$$

4. Numerical Comparisons and Calibration. We have derived approximate formulas for the probability density function and for the prices of European call and put options under the CEV and SABR models. When $\beta < 0$, our results for $c(F,t)$ and $p(F,t)$ are consistent with the put-call parity as well as Black's pricing formulas. For the CEV model, $p(\widehat{F},T,F,t)$ reduces to the result for the GBM if $\beta \to 0$ and to the Bachelier model if $\beta = -1$. For the SABR model, $p^F(\widehat{F},T,F,t)$ also exhibits the same limiting behavior for β in addition to $\nu \to 0$ and $\rho = 0$. Results 1,3,8 and 9 for the CEV and SABR models provide analytic approximations for the density function and pricing exhibiting deterministic and stochastic volatility. This demonstrates that it is possible to derive analytic approximations that can incorporate more *stylized facts* [10] about the behavior of the underlying asset, thus providing a more realistic view of the price of a derivative.

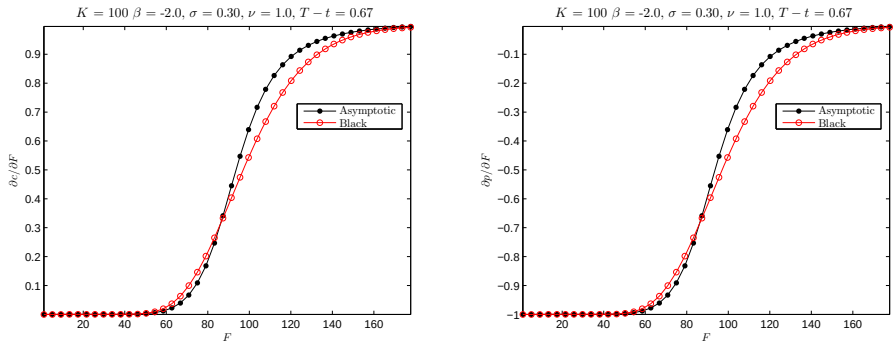

FIG. 3.4. *Illustration of the delta for the call and put price using (3.54) and (3.56) with parameters* $\beta = -2$, $K = 100$, $V = 0.3$, $\nu = 1.0$, $r = 0.0$ *and* $T - t = 3/4$ *versus the delta under Black's model.*

The asymptotic formulas for the price of European options under the CEV and SABR process, in Results 3 and 9, illustrate the strengths of the asymptotic method. As we demonstrate below these asymptotic approximations are very accurate so they can be used instead of the standard numerical methods. Such analytical approximations become quite useful in the exchange traded options world since the highest liquidity resides in contracts near expiration with a maturity of at most one year. Finally, we note that perturbation methods have be applied directly on the pricing PDEs in (2.2) and (3.2) [20, 22] though in different asymptotic limits.

To assess the usefulness of our formulas we will compare our results with available exact solutions as well as to numerical approximations to the exact solutions. Therefore we also use the numerical result as exact in determining the error. For the CEV model, the exact formula in (2.4) provides the benchmark for comparing the accuracy of the asymptotic approximation of the density in Result 1. The density function (2.13) is illustrated in Figure 4.1 where the leading term asymptotic approximation (2.13) for the density function p is compared to the exact solution in (2.4), for $\beta = -2$, $V = 0.4$, $T - t = 0.5$ and $\beta = 2$, $V = 0.4$, $T - t = 0.5$.

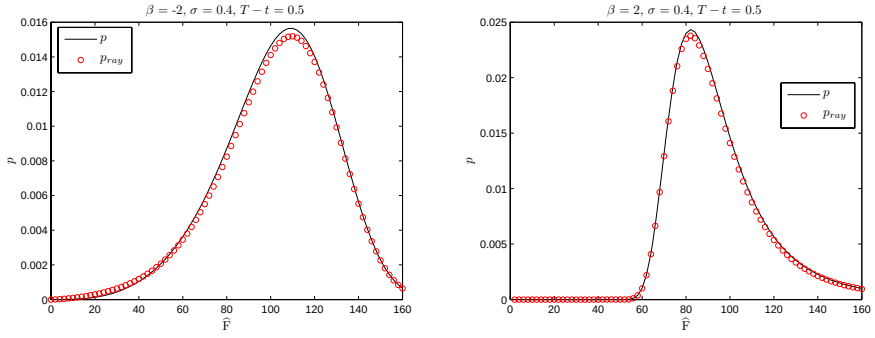

FIG. 4.1. *The two figures illustrate the leading term in (2.13) for the density function* p *and the exact solution in (2.4), for* $\beta = -2$, $V = 0.4$, $T - t = 0.5$ *(left plot) and* $\beta = 2$, $V = 0.4$, $T - t = 0.5$ *(right plot).*

We consider the ray solution (3.29) with $\beta = -1$ for the SABR model in Figure 4.2 in which a slice of the density is compared with the integral form of the exact solution in (3.8) in the original variables. The integral was performed numerically in MATLAB© using the recursive adaptive Simpson quadrature which tries to approximate the integral to within an

error of 10^{-6}. Even with a time to expiry of 1 year, with $V = 0.33$ and $\widehat{F} \in [10, 190]$ the maximum relative error is about 2.1%.

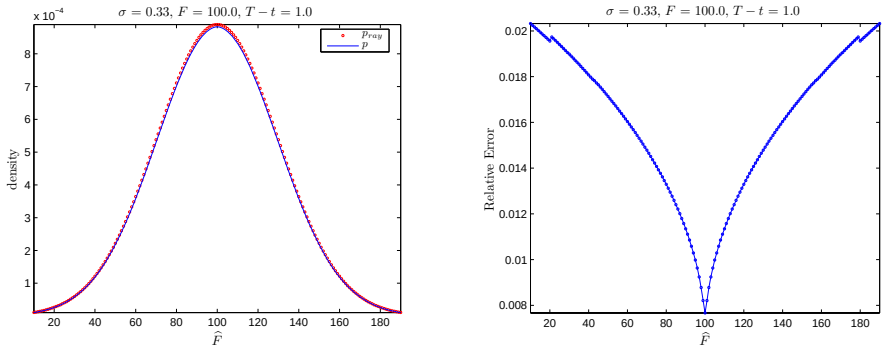

FIG. 4.2. *Comparison between the leading term ray solution for $\beta = -1$ in (3.29) and the numerical approximation of the exact solution of the McKean problem in (3.8) at $\sigma(F, t) = 0.33$ with $F = 100$ and $T - t = 1.0$.*

Figure 4.3 illustrates the approximation of the marginal density p^F for the SABR model and the exact solution in (3.13) with parameters $\beta = -1$, $\nu = 0$ and $\rho = 0$. Note that marginal density consists of integrating the density with respect to the variable $\widehat{V}$. One would expect from a second approximation the introduction of more residual error. However, since this is an asymptotic approximation, the error does not necessarily increase. In this case, the relative error actually decreases. Even with a time to expiry of 1 year, with $V = 0.33$ and $\widehat{F} \in [10, 190]$ the maximum relative error is less than 1%. The marginal density is used in the derivation of the pricing formulas in (3.48), (3.50), (3.51) and (3.52) in Result 9.

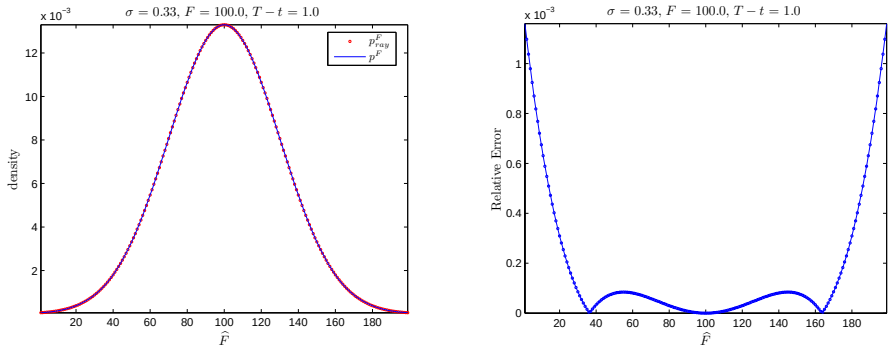

FIG. 4.3. *Comparison between the leading term ray solution for $\beta = -1$, $\rho = 0$ and $\nu = 0$ in (3.41) and the exact solution (3.13) with $\sigma(F, t) = 0.33$, $F = 100$ and $T - t = 1.0$.*

We illustrate the new pricing formulas for pricing European call options based on the CEV model for $\beta < 0$. Figure 4.4 compares the asymptotic approximation (2.33) from Result 3 to a numerical calculation of the exact integral representation in (2.26) as well as to the Black's pricing formula [5]. We selected the following parameters: $\beta = -2$, $V = 0.3$, $T - t = 0.5$ and $F = 100$. For the numerical integration we use the adaptive Simpson quadrature available in MATLAB©. With a maturity of half a year and $K \in [50, 150]$, the maximum relative error is about 2.3%.

Similarly, we illustrate the pricing formulas for the SABR model in Result 9. Recall that implied volatility are just *"the wrong number to put in the wrong formula to get the right*

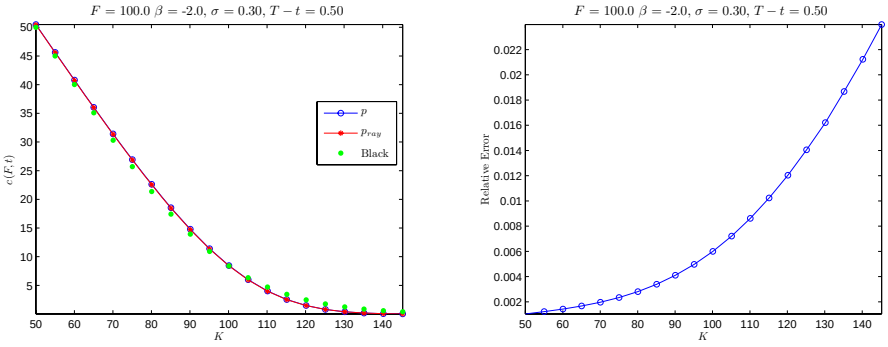

FIG. 4.4. *Comparison between the asymptotic pricing formulas for call options in (2.33) to numerical estimation of the exact integral representation in (2.25) and to Black's pricing formula. The selected parameters for the CEV model are* $\beta = -2$, $V = 0.3$, $T - t = 0.5$ *and* $F = 100$. *The relative error uses the numerical approximation as exact.*

price" [37], so there is no great meaning in obtaining implied volatilities rather than prices except for illustrating that a model captures some of the the stylized facts pertaining to implied volatility. However, the wrong number has become a common metric in some market places, such as the OTC market, to communicate the prices of options. In Figure 4.5 we illustrate that the asymptotic pricing formulas (3.48), (3.50), (3.51) and (3.52) capture the implied volatility smile or skew. Figure 4.5 illustrates the comparison between Black's, the CEV and the SABR implied volatilities. The CEV and SABR implied volatilities correspond to their respective asymptotic pricing formulas from Results 3 and 9. The deterministic and stochastic volatility models depart from the concept of constant implied volatility by exhibiting significant downward sloping volatility curves. Furthermore, depending on the model parameters the ITM and OTM options exhibit higher implied volatilities than ATM options, a common stylized fact in some markets.

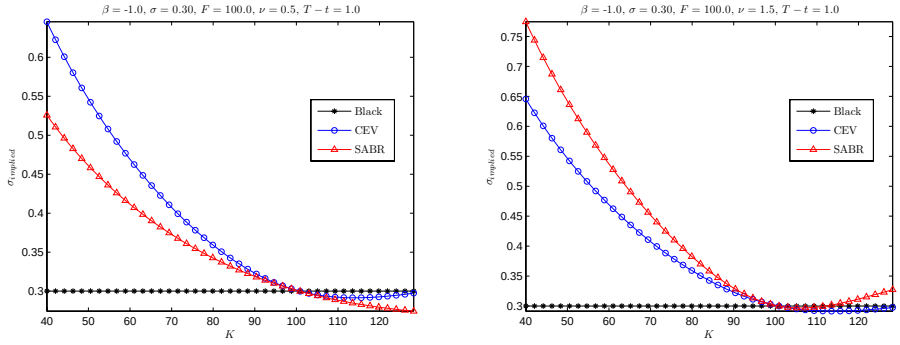

FIG. 4.5. *The two figures show a comparison of the implied volatility curves of Black's,* ($\beta = 0$, $\nu = 0$), *the CEV* ($\nu = 0$) *and the uncorrelated SABR model. The implied volatility curves correspond to prices generated from their respective models. The analytic pricing formulas in Result 3 and 9 were used for the CEV and SABR models, respectively. The parameters used are as follows:* $\beta = -1$ *with* $V = 0.3$, $T - t = 1$, $\nu = 0.5$ *(left plot) and* $\nu = 1.5$ *(right plot).*

We now illustrate the use of the new asymptotic formulas for the CEV and SABR models in calibrating to actual market data. In order to use Results 3 and 9 we demonstrate the ease of performing a simple calibration to liquid European option prices. The calibration consists

of identifying the parameters of the models from a set of observations of call and/or put option prices. In other words, finding the minimum of a function of one or more independent variables. In order to obtain a practical solution to the calibration problem, many practitioners minimize the function that represents the in-sample quadratic pricing error

$$\widetilde{\mathbf{p}} = \min_{\mathbf{p}} \sum_{i=1}^{N} |c_i(F,t) - c_i^m(F,t)|^2 \tag{4.1}$$

where N represents the in-sample size with the parameters are defined as $\mathbf{p} = (V)$, $\mathbf{p} = (V, \beta)$, and $\mathbf{p} = (V, \beta, \nu)$ for the Black, CEV and SABR models, respectively. Note that $\widetilde{\mathbf{p}}$ represents the estimation of $\mathbf{p}$ for the model under consideration. $c_i^m(F,t)$ is the market price of a call option observed at time t and $c_i(F,t)$ is the price of this option computed in a Black, CEV or SABR model with parameters $\mathbf{p}$ for strike K_i and maturity $\tau = T - t$, for $i = 1, \ldots, N$. The optimization problem (4.1) is usually solved numerically by a gradient-based method. However the minimization function is non-convex so a gradient descent may not succeed in locating the global minimum. In practice one needs to carefully take into account the potential reduction of the quality of the calibration algorithm, see for example [11].

In order to minimize the function (4.1) we use a Broyden-Fletcher-Goldfarb-Shanno (BFGS) gradient descent method (also referred to as a Quasi-Newton method)[36]. The essential step, beyond the determination of the initial guess $\mathbf{p}_0$, is the computation of the gradient of the function to be minimized with respect to the calibrated parameters using the analytical approximations in Result 3 and 9. The algorithm was written in C++ and all the calculations were performed on a Windows Vista™ operating system with 2.00 Ghz dual core CPU with 3.00 GB of memory.

TABLE 4.1

Calibration results given the simulated Call option prices with maturity $T - t = 0.25$ and given market option prices with maturity of 26 and 54 days. The true parameters used for the simulation are $\mathbf{p} = (0.4)$, $\mathbf{p} = (0.4, -2)$, and $\mathbf{p} = (0.4, -2, 1.5)$ for the Black, CEV and SABR models, respectively.

	Simulated Call Prices	Market Call Prices	
Calibrated Parameters	$T - t = 0.25$	$T - t = 26$ days	$T - t = 54$ days
BSM V	0.4000	0.1883	0.1847
BSM Minimization Score	0.0000	0.1514	0.3621
CEV V	0.4000	0.1914	0.1840
CEV β	-2.0000	-4.3404	-4.5734
CEV Minimization Score	0.0000	0.0145	0.1340
SABR V	0.4000	0.1889	0.1795
SABR β	-2.0000	-5.3446	-3.8098
SABR ν	1.5000	2.0972	1.5701
SABR Minimization Score	0.0000	0.0011	0.0836

To verify the accuracy and numerical stability of the our simple calibration, we tested it on simulated data sets of option prices generated using a Black, CEV and SABR model. We generated 21 call option prices with strikes ranging from 40 to 140 based on the Black, CEV and SABR models with a quarter of year to maturity. The spot price is set at 108.85

with risk free interest rate of 1%. The parameters used for the simulated prices are as follows: $\mathbf{p} = (0.4)$, $\mathbf{p} = (0.4, -2)$, and $\mathbf{p} = (0.4, -2, 1.5)$ for the Black, CEV and SABR models, respectively. We used the following initial guesses $\mathbf{p}_0 = (0.1)$, $\mathbf{p}_0 = (0.1, 0.1)$, and $\mathbf{p}_0 = (0.1, 0.1, 0.1)$. The calibration results from the simulation are available in Table 4.1. The algorithm recovers the correct parameters of the model despite the bad initial guesses. Next, we calibrated each of the models to one (26 days) and two (54 days) month European call option mid prices of the mini S&P 500 index (XSP index) traded on the Chicago Board of Option Exchange (CBOE). The result of the calibration are also available in Table 4.1. The minimization score in Table 4.1 consists of the sum of the absolute squared deviations away from the market prices, as suggested in equation (4.1). The closer the fit of the model to the observed data, the lower the score. The score can only be compared within a given data set. In other words, the minimization score for the shortest maturity cannot be compared to the second set because the data set is different. However, the scores for each model given the same data set are comparable. Note that all SABR calibrations are performed with elapsed times of less than 0.1 seconds.

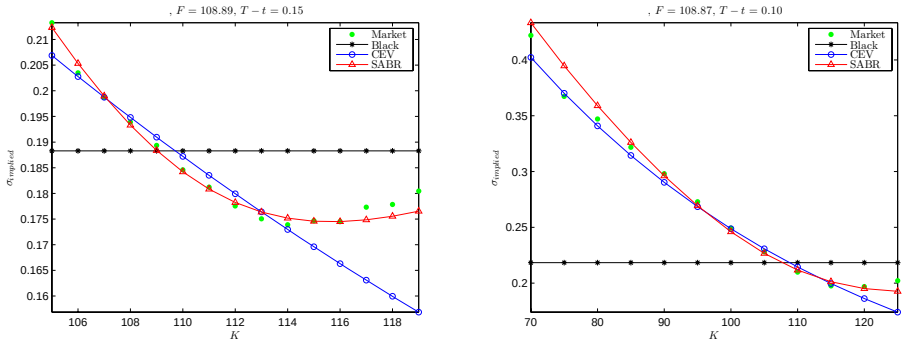

FIG. 4.6. *Implied volatility comparison using the leading term analytic pricing formula for the Black, CEV and SABR models calibrated to option prices with 26 days (left) and 54 days (right) to maturity. The calibrated parameters are available in Table 4.1.*

The illustration of the calibration in Table 4.1 is shown in Figure 4.6. Table 4.1 and Figure 4.6, show that the SABR model best fits the market prices compared to the Black and CEV model. The calibration results suggest the superiority of the SABR analytic formulas in capturing the smile or skew of the market implied volatility curve relative to the Black and CEV model. As suggested by the minimization scores.

Appendix A. Solution to Eikonal Equation.

The eikonal equation is

$$\widehat{x}^2 \left[\phi_{\widehat{y}}^2 + \phi_{\widehat{x}}^2 - 2\rho\phi_{\widehat{x}}\phi_{\widehat{y}} \right] = 1.$$

The characteristics, called rays, satisfy the differential equations

$$\begin{aligned} \frac{d\widehat{y}}{d\eta} &= \widehat{x}^2 \left[\phi_{\widehat{y}} - \rho\phi_{\widehat{x}} \right], \quad \frac{d\widehat{x}}{d\eta} = \widehat{x}^2 \left[\phi_{\widehat{x}} - \rho\phi_{\widehat{y}} \right], \\ \frac{d\phi_{\widehat{y}}}{d\eta} &= 0, \quad \frac{d\phi_{\widehat{x}}}{d\eta} = -\frac{1}{\widehat{x}}, \quad \frac{d\phi}{d\eta} = 1 \end{aligned} \tag{A.1}$$

with initial conditions

$$\widehat{y}(0) = y, \quad \widehat{x}(0) = x, \quad \phi_{\widehat{y}}(0) = p, \quad \phi_{\widehat{x}}(0) = q, \quad \phi(0) = 0. \tag{A.2}$$

Since the initial condition for the density is $\delta(x-\widehat{x})\delta(y-\widehat{y})$, we require the rays to emanate from this point parameterized by p and q such that

$$p=\theta\sin(\gamma),\qquad q=\theta\cos(\gamma),\qquad \theta=\frac{1}{x\sqrt{1-2\rho\cos(\gamma)\sin(\gamma)}}. \tag{A.3}$$

The value θ is chosen so that ϕ will be increasing with η and (3.18) holds at $\eta=0$. Therefore, for each angle γ we have a unique solution to (A.1) with (A.2) and (A.3), e.g. $\widehat{y}\equiv\widehat{y}(\eta,\gamma)$.

From (A.1) and (A.2) we solve (3.18). Since $\widehat{x}>0$, we use (3.18) to express $\widehat{x}$ with $\phi_{\widehat{y}}=p$. Then we substitute $\widehat{x}$ into (A.1) and solve, in this order, for $\phi_{\widehat{x}}$, $\widehat{x}$, $\widehat{y}$ and η. From the solution of $\widehat{x}$ we use (A.3) and a little algebra, to find the solution to the ray equations in (A.1) with initial conditions in (A.2) are given by

$$\begin{aligned}\widehat{x}(\eta)&=\frac{1}{p\sqrt{1-\rho^2}\cosh(\eta-\Psi)},\quad \widehat{y}(\eta)=\frac{1}{p}\tanh(\eta-\Psi)-\rho\widehat{x}+\frac{q}{p}x+y\\ \phi_{\widehat{x}}(\eta)&=p\left[\rho-\sqrt{1-\rho^2}\sinh(\eta-\Psi)\right],\quad \phi_{\widehat{y}}(\eta)=p,\quad \phi(\eta)=\eta,\end{aligned} \tag{A.4}$$

with

$$\Psi=\sinh\left(\frac{q-\rho p}{p\sqrt{1-\rho^2}}\right),\qquad \widehat{x}>0,\quad \eta>0,$$

so that

$$\phi\equiv\eta=\cosh^{-1}\left(1+\frac{(x-\widehat{x})^2+2\rho(x-\widehat{x})(y-\widehat{y})+(y-\widehat{y})^2}{2(1-\rho^2)\widehat{x}x}\right). \tag{A.5}$$

One can easily check that ϕ satisfies (3.18) and a special case appears in (3.10).

Appendix B. Solution to Transport Equation.

The transport equation is

$$\begin{aligned}\frac{dZ_0}{d\eta}+Z_0\Bigg[&\frac{1}{2}\widehat{x}^2\left(\phi_{\widehat{yy}}+\phi_{\widehat{xx}}-\rho\phi_{\widehat{xy}}-\rho\phi_{\widehat{yx}}\right)-\\ &\frac{\widehat{x}^2(\beta+1)}{2\widehat{y}\beta}\phi_{\widehat{y}}-\frac{\widehat{x}^2(\beta+1)}{\widehat{y}\beta}\left(\phi_{\widehat{y}}-\rho\phi_{\widehat{x}}\right)+2\widehat{x}\left(\phi_{\widehat{x}}-\rho\phi_{\widehat{y}}\right)-\frac{1}{2\phi}\Bigg]=0.\end{aligned}$$

From (A.1) we use the following relationship

$$\frac{1}{J}\frac{dJ}{d\eta}=\left[\left(\frac{d\widehat{x}}{d\phi}\right)_{\widehat{x}}+\left(\frac{d\widehat{y}}{d\phi}\right)_{\widehat{y}}\right]$$

where J is the Jacobian of the transformation from ray coordinates (η,γ) to space coordinates (x,y). Let $|a|$ represents the determinant of the infinitesimal covariance matrix a from the system in (3.1) times a factor of $1/2$ defined as

$$a=\frac{1}{2}\begin{bmatrix}V^2F^{2\beta+2} & \rho\nu V^2F^{\beta+1}\\ \rho\nu V^2F^{\beta+1} & \nu^2V^2\end{bmatrix}.$$

We also have the following relationship

$$\frac{1}{|a|}\frac{d|a|}{d\eta}=\frac{4}{\widehat{x}}\frac{d\widehat{x}}{d\eta}-\frac{2(\beta+1)}{\widehat{y}\beta}\frac{d\widehat{y}}{d\eta}$$

with respect to the transformed variables $\widehat{y}$ and $\widehat{x}$. Here the determinant $|a| \geq 0$. Thus (3.19) can be written is terms of the ray variables as

$$\begin{aligned}(\text{B.1}) \quad & \frac{dZ_0}{d\eta} \\ & + Z_0 \left[\frac{1}{2J}\frac{dJ}{d\eta} - \frac{1}{\widehat{x}}\frac{d\widehat{x}}{d\eta} - \frac{(\beta+1)}{2\widehat{y}\beta}\frac{d\widehat{y}}{d\eta} + \frac{1}{2|a|}\frac{d|a|}{d\eta} - \frac{1}{2\eta} - \frac{\rho\widehat{x}^2(\beta+1)\phi_{\widehat{x}}}{2\widehat{y}\beta} \right] = 0.\end{aligned}$$

After solving (B.1), the general solution of the ray solution can be expressed as

$$\begin{aligned}(\text{B.2}) \quad p_{ray} = Z_0(0,\gamma) e^{-\eta^2/2\nu^2\tau} \sqrt{\frac{\eta}{|a|J}} \left(\frac{\widehat{x}}{\widehat{y}^{-(\beta+1)/(2\beta)}} \right) \\ \times \exp\left(-\frac{\rho(\beta+1)}{2\beta} \int_0^\eta \frac{\widehat{x}^2(z)\phi_{\widehat{x}}(z)}{\widehat{y}(z)} dz \right)\end{aligned}$$

where

$$|a| = \frac{\nu^6 \widehat{x}^4 (1-\rho^2)}{4(\widehat{y}\beta)^{2(1+1/\beta)}} \quad \text{and} \quad \frac{\widehat{x}}{\sqrt{J}} = \sqrt{\frac{1 - 2\rho\sin(\gamma)\cos(\gamma)}{(1-\rho^2)\sinh(\eta)}}.$$

We carefully determine $Z_0(0,\gamma)$ by normalizing p_{ray} such that the initial condition is satisfied, i.e. $\lim_{\tau\to 0} p_{ray} = \delta(\widehat{x}-x)\delta(\widehat{y}-y)$. We find after a short calculation that

$$Z_0(0,\gamma) = -\frac{\nu}{4\pi\sqrt{1-2\rho\sin(\gamma)\cos(\gamma)}},$$

using the Taylor expansion around the points $\widehat{y} = y$ and $\widehat{x} = x$

$$\eta^2 \approx \frac{(\widehat{x}-x)^2}{(1-\rho^2)^2 x^2} + \frac{2\rho(\widehat{x}-x)(\widehat{y}-y)}{(1-\rho^2)^2 x^2} + \frac{(\widehat{y}-y)^2}{(1-\rho^2)^2 x^2} \quad \text{and} \quad \frac{\sinh(\eta)}{\eta} \approx 1.$$

Appendix C. Calculation of $\int_0^\phi H(z)dz$.

The leading term of the ray solution is

$$p_{ray} = -\frac{e^{-\phi^2/2\nu^2\tau}}{2\pi\tau\widehat{x}^2\nu^2\sqrt{1-\rho^2}} \sqrt{\frac{\phi}{\sinh(\phi)}} \left(\frac{\widehat{y}}{y}\right)^{(\beta+1)/(2\beta)} \exp\left[-\frac{\rho(\beta+1)}{2\beta} \int_0^\phi H(z)dz \right],$$

where ϕ is defined in (A.4) and

$$(\text{C.1}) \qquad H(z) \equiv \frac{\widehat{x}^2(z)\phi_{\widehat{x}}(z)}{\widehat{y}(z)}.$$

We find that $H(z)$ can be decomposed into

$$\begin{aligned}(\text{C.2}) \qquad H(z) = & \frac{1}{\sqrt{1-\rho^2}\cosh(z-\Psi)} + \\ & \frac{qx+py}{\rho - \sinh(z-\Psi) - (qx+py)\sqrt{1-\rho^2}\cosh(z-\Psi)}\end{aligned}$$

by using (A.4) in (C.2). Integrating (C.2) from zero to ϕ leads to

$$\int_0^{\phi} H(z)dz = \frac{2}{\sqrt{1-\rho^2}}\left\{\tan^{-1}\left(e^{\Psi}\right) - \tan^{-1}\left(e^{-\phi+\Psi}\right)\right\} + \frac{2}{\sqrt{(qx+py)^2(1-\rho^2)-1}}$$

$$\times\left\{\tan^{-1}\left(\frac{\left((qx+py)\sqrt{1-\rho^2}+\rho\right)\tanh(\Psi/2)-\sqrt{1-\rho^2}}{\sqrt{(qx+py)^2(1-\rho^2)-1}}\right)\right. \tag{C.3}$$

$$\left.\tan^{-1}\left(\frac{\left((qx+py)\sqrt{1-\rho^2}+\rho\right)\tanh([-\phi+\Psi]/2)-\sqrt{1-\rho^2}}{\sqrt{(qx+py)^2(1-\rho^2)-1}}\right)\right\}.$$

(C.4)

Converting back to the (x, y) variables we use the identity

$$\frac{q}{p} = \frac{x^2-\widehat{x}^2-(y-\widehat{y})^2+2\widehat{x}\rho(y-\widehat{y})}{2x[\rho(x-\widehat{x})+(y-\widehat{y})]} \tag{C.5}$$

in combination with (A.4) and find

$$\begin{aligned} qx+py = \frac{1}{\sinh(\phi)}\left\{y[\rho(x-\widehat{x})+(y-\widehat{y})]\right. \\ \left.-\widehat{x}\rho(y-\widehat{y})-\left[\frac{x^2-\widehat{x}^2-(y-\widehat{y})^2}{2}\right]\right\} \end{aligned} \tag{C.6}$$

and

$$\begin{aligned} \Psi &= \sinh^{-1}\left(\frac{q-p\rho}{\sqrt{1-\rho^2}}\right) \\ &= \sinh^{-1}\left(\frac{1}{\sqrt{1-\rho^2}}\left[\frac{x^2-\widehat{x}^2-(y-\widehat{y})^2-2\rho(y-\widehat{y}+\rho)(x-\widehat{x})}{2x[\rho(x-\widehat{x})+(y-\widehat{y})]}\right]\right) \end{aligned} \tag{C.7}$$

with ϕ defined in (A.4) using (3.20).

Appendix D. Boundary Layer Solution.

Substituting (3.34) into (3.31) we find the leading order boundary layer equation to be

$$\left[\widehat{\xi}\Psi\right]_{\widehat{\xi}\widehat{\xi}} - \left\{\left[\left(1+\frac{1}{2\beta}\right)\right]\Psi\right\}_{\widehat{\xi}} + \left[\frac{\nu^2\theta^2_{\widehat{V}}}{4} - \frac{\theta}{2\widehat{V}^2}\right]\Psi = 0, \quad \beta < 0,\ \rho = 0, \tag{D.1}$$

with initial condition $\Psi(0) = 0$. The general solution is

$$\Psi(\widehat{\xi}) = C_1\widehat{\xi}^{(1-\beta)/4\beta}M\left(0, \frac{1}{2|\beta|}, 2\sqrt{(2\theta/\widehat{V}^2 - \nu^2\theta^2_{\widehat{V}})}\sqrt{\widehat{\xi}}\right) \tag{D.2}$$

where $M = M(\cdot,\cdot,z)$ is the Whittaker hypergeometric function and C_1 is a constant. The leading term of the boundary layer solution is of the form

$$p_b = C_1\tau^{1/2\beta+1/2}\widehat{\xi}^{(1-\beta)/[4\beta]}e^{-\theta/\tau}M\left(0, \frac{1}{2|\beta|}, 2\sqrt{(2\theta/\widehat{V}^2 - \nu^2\theta^2_{\widehat{V}})}\sqrt{\widehat{\xi}}\right) \tag{D.3}$$

where C_1 is the normalization constant to be determined from matching. The matching consists of comparing p_b for $\widehat{\xi} \to \infty$ with p_{ray} given $\widehat{y} \to 0$ and choosing the unknown constants so that the two expressions are the same.

From [21], we know that $M(\nu,\mu,z) \sim \Gamma(2\mu+1)z^{-\nu}e^{z/2}/\Gamma(\mu-\nu+1/2)(1+\ldots)$ for $z \gg 1$ which implies that as $\widehat{\xi} \to \infty$ that

$$\begin{aligned} p_b = & C_1 \tau^{1/2\beta+1/2} \frac{\Gamma\left(\frac{1}{|\beta|}+1\right)\widehat{\xi}^{(1-\beta)/4\beta}}{\Gamma\left(\frac{1}{2|\beta|}+\frac{1}{2}\right)} \\ & \times \exp\left(-\frac{\theta}{\tau}+\sqrt{\widehat{\xi}}\left[\sqrt{\frac{2\theta}{\widehat{V}^2}-\nu^2\theta_{\widehat{V}}^2}\right]\right)(1+\ldots), \quad \widehat{\xi}\to\infty. \end{aligned}$$

We re-write the boundary layer solution in terms of $\widehat{y}$

$$\begin{aligned} p_b = & \frac{C_1}{\tau}\frac{\Gamma\left(\frac{1}{|\beta|}+1\right)\widehat{y}^{(1-\beta)/4\beta}}{\Gamma\left(\frac{1}{2|\beta|}+\frac{1}{2}\right)} \\ & \times \exp\left(-\frac{\theta}{\tau}+\frac{\sqrt{\widehat{y}}}{\tau}\left[\sqrt{\frac{2\theta}{\widehat{V}^2}-\nu^2\theta_{\widehat{V}}^2}\right]\right)(1+\ldots), \quad \tau\to 0. \end{aligned} \tag{D.4}$$

We then compare (D.4) to the leading term (3.32) for $\widehat{y} \to 0$

$$p_{ray} \sim \frac{e^{-\phi_0^2/2\nu^2\tau+\frac{\sqrt{\widehat{yy}}}{V\widehat{V}\tau}\left(\frac{\phi_0}{\sinh(\phi_0)}\right)}}{4\pi\tau\nu\widehat{V}^2\sqrt{\widehat{y}}}\sqrt{\frac{\phi_0}{\sinh(\phi_0)}}\left(\frac{\widehat{y}}{y}\right)^{(\beta+1)/(4\beta)}, \tag{D.5}$$

for which we find, after matching

$$\theta = \frac{\phi_0^2}{2\nu^2}, \qquad \text{and} \qquad \theta_{\widehat{\mathrm{V}}} = \frac{\phi_0\phi_{0,\widehat{\mathrm{V}}}}{\nu^2},$$

where

$$\phi = \cosh^{-1}\left(1+\frac{(V-\widehat{V})^2+\nu^2(y^{1/2}-\widehat{y}^{1/2})^2}{2V\widehat{V}}\right) \tag{D.6}$$

and

$$\phi_0 = \phi|_{\widehat{\xi}=0} = \cosh^{-1}\left(1+\frac{(V-\widehat{V})^2+\nu^2 y}{2V\widehat{V}}\right).$$

In addition we have

$$\phi^2 \sim \phi_0^2 - 2\nu^2\tau^2\frac{\sqrt{\xi\widehat{\xi}}}{V\widehat{V}}\left(\frac{\phi_0}{\sinh(\phi_0)}\right)$$

and

$$\phi_0^2\left(\frac{1}{\widehat{V}^2}-\phi_{0,\widehat{V}}^2\right) = \frac{\tau^2\nu^2\xi}{(V\widehat{V})^2}\left(\frac{\phi_0}{\sinh(\phi_0)}\right)^2. \tag{D.7}$$

This leads to solving for C_1

$$C_1 = \frac{y^{-(\beta+1)/[4\beta]}}{4\pi\nu\widehat{V}^2}\left(\frac{\Gamma(1/2|\beta|+1/2)}{\Gamma(1/|\beta|+1)}\right)\sqrt{\frac{\phi_0}{\sinh(\phi_0)}}.$$

Substituting C_1 back in (D.3) leads to

$$\begin{aligned} p_b = \frac{(\widehat{y}y)^{-1/4}}{4\pi\tau\nu\widehat{V}^2}\left(\frac{\Gamma(1/2|\beta|+1/2)}{\Gamma(1/|\beta|+1)}\right)\sqrt{\frac{\phi_0}{\sinh(\phi_0)}}\left(\frac{\widehat{y}}{y}\right)^{1/4\beta} e^{-\phi_0^2/2\nu^2\tau} \\ \times M\left(0,\frac{1}{2|\beta|},\frac{2}{\tau V\widehat{V}}\left(\frac{\phi_0}{\sinh(\phi_0)}\right)\sqrt{y\widehat{y}}\right). \end{aligned} \tag{D.8}$$

We use the following relationship[2] between the modified Bessel function $I_\nu(z)$ and the special Whittaker hypergeometric function $M(0,\cdot,z)$

$$M(0,\mu,z) = 4^\mu\sqrt{z}\Gamma(\mu+1)I_\mu\left(\frac{z}{2}\right).$$

leading to

$$\begin{aligned} p_b = \frac{2^{1/|\beta|}e^{-\phi_0^2/2\nu^2\tau}}{2\sqrt{2}\pi\tau^{3/2}\widehat{V}^2\nu\sqrt{V\widehat{V}}}\left(\frac{\Gamma(1/2|\beta|+1)\Gamma(1/2|\beta|+1/2)}{\Gamma(1/|\beta|+1)}\right) \\ \times\left(\frac{\phi_0}{\sinh(\phi_0)}\right)\left(\frac{\widehat{y}}{y}\right)^{1/4\beta} I_{1/2|\beta|}\left(\frac{1}{\tau V\widehat{V}}\left(\frac{\phi_0}{\sinh(\phi_0)}\right)\sqrt{y\widehat{y}}\right) \end{aligned} \tag{D.9}$$

and

$$\frac{\Gamma(1/2|\beta|+1)\Gamma(1/2|\beta|+1/2)}{\Gamma(1/|\beta|+1)} = \frac{\sqrt{\pi}}{2^{1/|\beta|}}$$

where we used the identities $\Gamma(x+1) = x\Gamma(x)$ and Legendre duplication formula[3] $\Gamma(2x) = 2^{2x-1/2}\Gamma(x)\Gamma(x+1/2)/\sqrt{2\pi}$. As such (D.9) simplifies to

$$p_b = \frac{e^{-\phi_0^2/2\nu^2\tau}}{2\sqrt{2\pi}\tau^{3/2}\widehat{V}^2\nu\sqrt{V\widehat{V}}}\left(\frac{\phi_0}{\sinh(\phi_0)}\right)\left(\frac{\widehat{y}}{y}\right)^{1/4\beta} I_{1/2|\beta|}\left(\frac{1}{\tau V\widehat{V}}\left(\frac{\phi_0}{\sinh(\phi_0)}\right)\sqrt{y\widehat{y}}\right).$$

Appendix E. Marginal Density Function.

The asymptotic formula for the marginal density function $p^F_{ray} = p^F_{ray}(\widehat{F},T,F,t)$ can be represented as

$$p^F_{ray} = \frac{1}{2\pi\nu(T-t)\widehat{F}^{\beta+1}}\left(\frac{\widehat{F}}{F}\right)^{-(\beta+1)/2}\int_0^\infty \frac{1}{\widehat{V}^2}\sqrt{\frac{\phi}{\sinh(\phi)}}e^{g(\widehat{V})/(T-t)}d\widehat{V},$$

where $g(\widehat{V}) = -\phi^2/2\nu^2$ and ϕ defined in (3.24). The integral in p^F_{ray} is a Laplace type integral so we will expand it for $T-t \ll 1$. We find that $g(\widehat{V})$ has an interior maximum point at

$$\widehat{V}_{\max} = \sqrt{V^2 + \frac{\nu^2}{\beta^2}(F^{-\beta}-\widehat{F}^{-\beta})^2}$$

[2] http:\\functions.wolfram.com: 07.44.03.0010.01
[3] http:\\functions.wolfram.com: 06.05.16.0006.01

for which $\dfrac{\partial g}{\partial \widehat{V}} = 0$, $\dfrac{\partial^2 g}{\partial \widehat{V}^2} < 0$ and $g(\widehat{V}) \neq 0$. We can approximate p^F in the neighborhood of $\widehat{V}_{\max}$ by the following leading term

$$p^F \sim \frac{1}{2\pi\nu(T-t)\widehat{F}^{\beta+1}} \left(\frac{\widehat{F}}{F}\right)^{-(\beta+1)/2} \frac{\sqrt{2\pi} e^{g(\widehat{x}_{\max})/(T-t)}}{\sqrt{-g''(\widehat{x}_{\max})/(T-t)}} \frac{1}{\widehat{V}^2} \sqrt{\frac{\phi}{\sinh(\phi)}}, \qquad T-t \to 0,$$

where

$$g(\widehat{x}_{\max}) = -\frac{\phi_{\max}^2}{2\nu^2}$$

with $\phi_{\max} = \cosh^{-1}\left(\widehat{V}_{\max}/V\right)$. We also find that

$$g''(\widehat{V}_{\max}) = -\frac{\phi_{\max}}{\widehat{V}_{\max}\sqrt{\widehat{V}_{\max}^2 - V^2}}$$

where $\sinh(\cosh^{-1}(x)) = \sqrt{x^2-1}$, leading to

$$p^F \sim \frac{e^{-\phi_{\max}^2/2\nu^2(T-t)}}{\sqrt{2\pi(T-t)}\widehat{V}_{\max}\widehat{F}^{\beta+1}} \sqrt{\frac{V}{\widehat{V}_{\max}}} \left(\frac{\widehat{F}}{F}\right)^{-(\beta+1)/2}, \qquad T-t \to 0.$$

REFERENCES

[1] C. ALBANESE AND G. CAMPOLIETI, *Advanced Derivatives Pricing and Risk Management*, Elsevier Academic Press, 1st ed., 2006.

[2] C. ALBANESE, G. CAMPOLIETI, P. CARR, AND A. LIPTON, *Black-Scholes goes Hypergeometric*, Risk, 14 (2001), pp. 99–103.

[3] L. ANDERSEN AND J. ANDREASEN, *Volatility skews and extensions of the LIBOR market model*, Applied Mathematical Finance, 7 (2000), pp. 1–32.

[4] L. ANDERSEN AND R. BROTHERTON-RATCLIFFE, *Extended LIBOR market models with stochastic volatility*, Journal of Computational Finance, 9 (2005), pp. 1–40.

[5] F. BLACK, *Studies of stock price volatility changes*, Proceedings of the 1976 Meetings of the American Statistical Association, (1976), pp. 177–181.

[6] FISHER BLACK AND MYRON SCHOLES, *The pricing of options and corporate liabilities*, Journal of Political Economy, 81 (1973), pp. 637–654.

[7] P. CARR AND V. LINETSKY, *A jump to default extended CEV model*, Finance and Stochastics, 10 (2006), pp. 303–330.

[8] A. CHIRSTIE, *The stochastic behavior of common stock variances*, Journal of Financial Economics, 10 (1982), pp. 407–432.

[9] J.K. COHEN AND R.M. LEWIS, *A ray method for the asymptotic solution of the diffusion equation*, Journal of the Institute of Mathematics and Its Applications, 3 (1967), pp. 266–290.

[10] R. CONT, *Empirical properties of of asset returns: Stylized facts and statistical issues*, Quantitative Finance, 1 (2001), pp. 223–236.

[11] R. CONT AND P. TANKOV, *Non-parametric calibration of jump-diffusion option models*, The Journal of Computational Finance, 7 (2004), pp. 1–49.

[12] J. COX, *The constant elasticity of variance option pricing model*, Journal of Portfolio Management, 22 (1996), pp. 5–17.

[13] J. COX AND S. ROSS, *The valuation of options for alternative stochastic processes*, Journal of Financial Economics, 3 (1975), pp. 145–166.

[14] D. DAVYDOV AND VADIM LINETSKY, *Pricing and hedging path-dependent options under the CEV process*, Management Science, 47 (2001), pp. 949–965.

[15] ———, *Pricing options on scalar diffusions: An eigenfunction expansion approach*, Operations Research, 51 (2003), pp. 185–209.

[16] E. DERMAN, I . KANI, AND N. CHRISS, *Implied trinomial trees of the volatility smile*, Journal of Derivatives, 4 (1996).

[17] B. DUPIRE, *Model art*, RISK, Sept (1993), pp. 118–120.
[18] ———, *Pricing with a smile*, RISK, Jan (1994), pp. 18–20.
[19] D. EMANUEL AND D. MACBETH, *Further results on the constant elasticity of variance call option pricing model*, Journal of Financial and Quantitative Analysis, 17 (1982), pp. 533–554.
[20] J.-P. FOUQUE, G. PAPANICOLAOU, AND K.R. SIRCAR, *Derivatives in Financial Markets with Stochastic Volatility*, Canbridge University Press, 1^{st} ed., 2000.
[21] I.S. GRADSHTEYN AND I.M. RYZHIK, *Table of Integrals, Series, and Products*, Academidc Press, 4^{th} ed., 1980.
[22] P. HAGAN, D. KUMAR, A. LESNIEWSKI, AND D. WOODWARD, *Managing smile risk*, Wilmott Magazine, Sept (2002), pp. 84–108.
[23] P. HAGAN, A. LESNIEWSKI, AND D. WOODWARD, *Probability distribution in the SABR model of stochastic volatility*. Working Paper, June 2004.
[24] P. HAGAN AND D. WOODWARD, *Equivalent Black volatilities*, Applied Mathematical Finance, 6 (1999), pp. 147–157.
[25] PIERRE HENRY-LABORDÈRE, *A general asymptotic implied volatility for stochastic volatility models*. Working Paper, Draft of May 2005, May 2005.
[26] S. HESTON, *A closed form solution for options with stochastic volatility with applications to bond and currency options*, Review of Financial Studies, 6 (1993), pp. 327–343.
[27] S. HOWISON, *A matched asymptotic expansion approach to continuity corrections for discretly sampled options. part 2: Bermudan options*, Applied Mathematical Finance, 14 (2007), pp. 91–104.
[28] J. HULL AND A.D. WHITE, *The pricing of options on assets with stochastic volatilities*, Journal of Finance, 42 (1987), pp. 281–300.
[29] R. JORDAN, *Asymptotic Approximations to Fundamental Solutions with Applications to Financial Derivatives*, Ph.D., Department of Mathematics, University of Illinois at Chicago, 2008.
[30] R. JORDAN AND C. TIER, *The variance swap contract under the CEV process*, International Journal of Theoretical and Applied Finance, 12 (2009), pp. 709–743.
[31] J. KELLER, *Rays, waves and asymptotics*, Bulletin of the American Mathematical Society, 84 (1978), pp. 727–750.
[32] ANDREW LESNIEWSKI, *WKB method for swaption smile*. Working Paper, February 2002.
[33] A. LEWIS, *Option Valuation under Stochastic Volatility with Mathematica Code*, Finance Press, 1^{st} ed., 2000.
[34] A. LIPTON, *Mathematical Methods for Foreign Exchange*, World Scientific, 1^{st} ed., 2001.
[35] H.P. MCKEAN, *An upper bound to the spectrum of $\triangle$ on a manifold of negative curvature*, Journal of Differential Geometry, 4 (1970), pp. 359–366.
[36] W. PRESS, S. TEUKOLSKY, W. VETTERLING, AND B. FLANNERY, *Numerical Recipes in C: The Art of Scientific Computing*, Cambridge University Press, 2^{nd} ed., 1992.
[37] R. REBONATO, *Volatility and Correlation: The Perfect Hedger and the Fox*, John Wiley & Sons, Ltd., 2^{nd} ed., 2004.
[38] R. REBONATO, K. MCKAY, AND R. WHITE, *The SABR/LIBOR Market Model*, Wiley, 1^{nd} ed., 2009.
[39] N. M. TEMME, *The uniform asymptotic expansion of a class of integrals related to cumulative distribution functions*, SIAM Journal of Mathematical Analysis, 13 (1982), pp. 239–253.
[40] C. TIER, *An analysis of neutral-alleles and variable-environement diffusion models*, Journal of Mathematical Biology, 12 (1981), pp. 53–71.
[41] C. TIER AND J. KELLER, *Asymptotic analysis of diffusion equations*, SIAM Journal of Applied Mathematics, 34 (1978), pp. 549–576.
[42] ———, *A tri-allelic diffusion model with selection*, SIAM Journal of Applied Mathematics, 35 (1978), pp. 521–535.
[43] S.R.S. VARADHAN, *Diffusion processes in a small time interval*, Communications on Pure and Applied Mathematics, 20 (1967), pp. 659–685.
[44] L. WU AND F. ZHANG, *Fast swaption pricing under the market model with with a square-root volatility process*, Quantitative Finance, 8 (2008), pp. 163–180.